Savolainen, Rebecka; Einolander, Johannes; Lahdelma, Risto

Optimizing building hybrid energy systems for demand response marketplace operation

Published in:
Journal of Energy Storage

DOI:
10.1016/j.est.2024.114108

Published: 15/11/2024

Document Version
Publisher's PDF, also known as Version of record

Please cite the original version:
Savolainen, R., Einolander, J., & Lahdelma, R. (2024). Optimizing building hybrid energy systems for demand response marketplace operation. *Journal of Energy Storage*, *102*, Article 114108.
https://doi.org/10.1016/j.est.2024.114108

Journal of Energy Storage 102 (2024) 114108

Contents lists available at ScienceDirect

Journal of Energy Storage

journal homepage: www.elsevier.com/locate/est

Research papers

Optimizing building hybrid energy systems for demand response marketplace operation

Rebecka Savolainen [a,b,d,*], Johannes Einolander [a], Risto Lahdelma [a,c]

[a] *Aalto University, School of Engineering, Department of Mechanical Engineering, Otakaari 4, FIN-02150 ESPOO, Finland*
[b] *Tallinn University of Technology (TalTech), School of Engineering, Department of Electrical Power Engineering and Mechatronic, Ehitajate tee 5, 19086 TALLINN, Estonia*
[c] *Aalto University, School of Science, Department of Mathematics and Systems Analysis, Otakaari 1, FIN-02150 ESPOO, Finland*
[d] *Granlund Oy, Malminkaari 21, FIN-00701, Finland*

A R T I C L E I N F O

Keywords:
Demand response
District heating
Ground Source heat pump
Energy storage
Frequency containment reserve
Linear programming

A B S T R A C T

Increasing amounts of renewable power make it difficult to balance supply and demand in the grid. European Transmission System Operators invite consumers to participate in grid balancing through various demand response mechanisms. Individual buildings can contribute to grid balancing by reacting to dynamic electricity prices through implicit demand response. Buildings can also participate in explicit demand response programs, for instance through the Frequency Containment Reserve (FCR) market. This study presents a novel linear programming optimization model for implicit and explicit demand response operation of a building with a hybrid energy system including a ground source heat pump, district heating, power storage, heat storage, and which participates in the daily FCR market. The model is applied to the retrofit planning of an office building in subarctic Helsinki, Finland. The study compares four potential configurations, with and without power storage and with and without FCR trade. Results show that for the target building, FCR trade can save yearly about 3 % of the energy costs. Power storage was found to be cost-efficient only in conjunction with FCR trade.

1. Introduction

Increasing integration of intermittent renewable energy sources in the power systems makes it difficult to balance supply and demand in the grid [1]. As power production is becoming less controllable, demand needs to become more flexible through various demand response mechanisms [2,3]. Implicit demand response means that consumers are encouraged to adjust their demand in reaction to price signals, such as dynamic power pricing. Explicit demand response denotes committed, dispatchable consumer flexibility facilitated through a marketplace operated, for instance by a Transmission System Operator (TSO). Recently, European TSOs have invited consumers to participate in grid balancing through different explicit demand response mechanisms [4].

Lack of power production to match the momentary demand decreases the grid frequency, and similarly, excess production increases the frequency. European TSOs use five different mechanisms to balance the system and restore the nominal 50 Hz grid frequency: Frequency Containment Reserve (FCR), Imbalance Netting (IN), Frequency Restoration Reserves with automatic activation (aFRR), Frequency Restoration Reserves with manual activation (mFRR), and Replacement Reserves (RR) [3]. In addition to these reserves, fast frequency reserve (FFR) was introduced to the Nordics in 2020 to prevent low inertia situations [5,6]. FCR is an automatically activated power reserve that is used for constant control of grid frequency and quick disturbance response [7]. In the Nordic power system, TSOs use two different FCR resources: Frequency Containment Reserve for Normal Operation (FCR—N) also known as primary control reserve, and Frequency Containment Reserve for Disturbances (FCR—D) [8]. FCR-N is the first response to frequency deviations, used constantly to keep the grid frequency within 0.1 Hz from the nominal 50 Hz. The Finnish TSO, Fingrid, procures FCR resources from domestic yearly and hourly markets, and neighboring countries [9].

A relatively new group of consumers that can participate in the FCR-N market are buildings. Buildings can contain a wide variety of energy systems. In particular, buildings with hybrid energy systems including different forms of heat and electricity production and storage systems are interesting actors in the FCR-N capacity market, as the flexibility offered by the hybrid system allows consumption to be rapidly adjusted up and down without severe impacts to building operation or comfort.

* Corresponding author at: Malminkaari 21, FIN-00701, Finland.
E-mail addresses: rebecka.savolainen@gmail.com, rebecka.savolainen@granlund.fi (R. Savolainen).

https://doi.org/10.1016/j.est.2024.114108
Received 26 March 2024; Received in revised form 30 September 2024; Accepted 4 October 2024
Available online 18 October 2024

Nomenclature

Abbreviations

COP	The coefficient of performance of a heat pump
DH	District heating
DR	Demand response
FCR	Frequency Containment Reserve
FCR-D	Frequency Containment Reserve for Disturbances
FCR-N	Frequency Containment Reserve for Normal Operation
HP	Heat pump
HS	Heat storage
LP	Linear programming
MILP	Mixed integer linear programming
MW	Megawatt
MWh	Megawatt hour
PP	Power purchase from the grid
PS	Power storage

Indices and index sets

t	Time index (hour), $t = 1, \dots$ T
u	Index for energy supply and storage units
*	Superscript for the optimized value of decision variable
CONST	Superscript for constant cost term in the objective function
H	Sub/superscript referring to heat
MAX	Superscript for an upper bound of a variable
MIN	Superscript for the lower bound of a variable
P	Sub/superscript referring to electric power
S	Set of energy storages (heat, power)
U	Set of energy supply units (contracts or production units)

Symbols

$c_{u,t}$, €/MWh	Price coefficient for operation of energy supply unit u in period t
c_u^{MAX}, -	Price per capacity (annuity) for energy supply unit u (€/MW) or for storage u (€/MWh)
c_u^{CONST}, €	Constant term for the fixed costs (annuity) of energy supply unit u
c_t^{FCR}, €/MW	Market price on daily FCR-N market for capacity in period t
$x_{u,t}$, MW	Operating level of energy supply unit u in period t
$x_{HP,t}^{H}$, MW	Heat pump heat production rate in period t
x_u^{MAX}, MW	Capacity of energy supply unit u
E_t^{FCR}, MWh	Net FCR-N activation energy in period t
P_t^{FCR}, MW	Maximum FCR-N activation power in period t
$P_t^{FCR,BID}$, MW	Bid for FCR-N capacity in period t
$P_t^{FCR,HP}$, MW	Change in HP power due to FCR-N activation in period t
$P_t^{FCR,PS}$, MW	Change in PS net charge rate due to FCR-N activation in period t
$P_t^{FCR,X}$, MW	Unsupplied FCR-N capacity (activation power) in period t
$s_{u,t}$, MWh	Storage level of storage u at the end of period t
s_u^{MAX}, MWh	Storage capacity of storage u
$s_{u,t}^{IN}$, MW	Storage charge rate of storage u in period t
$s_u^{IN,MAX}$, MW	Storage maximum charge rate of storage u
$s_{u,t}^{OUT}$, MW	Storage discharge rate of storage u in period t
$s_u^{OUT,MAX}$, MW	Storage maximum discharge rate of storage u
T_t^{FCR}, h	Utilization period for maximum FCR-N activation in period t
η_u^S, 1	Storage efficiency of storage u, to model self-discharge per period
η_u^{IN}, 1	Efficiency for charging storage u
η_u^{OUT}, 1	Efficiency for discharging storage u
$\eta_{HP,t}$, 1	Heat pump efficiency (COP-factor)
σ_t, 1	Safety margin for FCR-N bidding in hour t of day

In this study, we consider a building with a hybrid energy system consisting of power purchase from the grid (PP), a ground source heat pump (HP), district heating (DH), power storage (PS), and heat storage (HS). We study the optimal sizing and operation of the hybrid energy system subject to dynamic power price and participation in the Finnish daily FCR-N market. We apply a novel linear programming (LP) model to an existing office building in the subarctic Helsinki, Finland. The presented methodology is general and can be applied to buildings with different energy technologies and energy forms in different climate zones.

1.1. Related research in the field and novelty of this study

Table 1 outlines various technologies and their applications in the context of Frequency Containment Reserves (FCR) and other ancillary service markets. The studies focused on different building energy loads and technologies [10–15], and the participation of specific technologies in FCR markets including their utilization, simulation, and optimization [7,16–33]. With rapid electrification, some studies explored using electric vehicles (EVs) for household or explicit demand response, treating EVs as power storage with limited availability. Other studies investigated the utilization and simulation of building energy loads for demand response in FCR, including elevators, escalators, battery storage systems, electric boilers, reused EV batteries, and combined heat and power facilities with PV and energy storage devices. One study focused on air-conditioning loads in buildings through demand-side management [44], while another proposed optimal demand-side management for EVs and energy storage systems (ESS) in grid-connected buildings. An optimization model for hybrid building energy systems in energy and ancillary service markets was also studied. Additionally, a joint-optimization method for household prosumers with PV, EV charging, batteries, and power converters was explored for improved economic feasibility in Spain [7]. A review of business models in Finnish pilot projects for FCR market participation highlighted the role of district heating in providing balancing services in the EU [34].

The related research articles cover the utilization of building energy loads for explicit demand response using various models and simulations, including the Shepherd model in MATLAB/Simulink for household-prosumer markets, two-stage optimization for industrial settings, and comprehensive reviews for non-residential buildings. Scenario-based stochastic [13] models were applied for the residential sector, and experimental simulations [14] were conducted for real buildings, such as a 12-story structure. Hybrid building energy systems were analyzed through real-time TRNSYS-MATLAB co-simulation [15] for day-ahead joint energy and ancillary service markets. District heating's potential contribution to FCR in EU countries was reviewed [33], and mixed-integer linear programming (MILP) models [18,24,29,33,39] were used for elevator and escalator energy loads [18,19]. Battery energy storage systems, electric boilers with battery storage [21–24,27,28], stationary battery systems, and reused EV batteries were also simulated for FCR market participation.

The studies explored optimization models for combined heat and power facilities with PV and energy storage devices, aggregated residential heat pumps, and hybrid battery systems in aFRR markets [30]. Virtual power plants [31] for distributed energy resources, scenarios for heat pumps in district heating [32], and the operation of district heating

Table 1
Main findings of the related research.

Reference / Year	Objective	The area of use and Methodology or/and Model	Location or Environment or Study Type
Hernandez J. C et al. [10]; 2019	The utilization and simulation of various building energy loads for explicit demand response in FCR	Household-prosumer market/Shepherd model for power storage	MATLAB/ Simulink environment
Urbano E.M et al. [11]; 2021	The utilization and simulation of various building energy loads for explicit demand response in FCR	Industrial settings / LP (two-stage optimization)	Analytical Study
Wang H et al. [12]; 2019	The utilization and simulation of various building energy loads for explicit demand response in FCR	Non-residential buildings	Hong Kong/ Comprehensive Review
Farrokhifar M et al. [13]; 2020	The utilization and simulation of various building energy loads for explicit demand response in FCR	The residential sector	Scenario-based stochastic model
Rotger-Griful S et al. [14]; 2016	The utilization and simulation of various building energy loads for explicit demand response in FCR	Real 12-storey building	Experimental simulation model
Tang H et al. [15]; 2021	The utilization and simulation of various building energy loads for explicit demand response in FCR	Hybrid building energy systems participating in day-ahead joint energy and ancillary service markets	California (United States) Real-time TRNSYS-MATLAB co-simulation
Ramos A et al. [16]; 2021	Review of different business models applied to various pilot projects that could participate in the FCR market	Buildings in Finland that could participate in the FCR market	Finland
Boldrini A et al. [17]; 2022	The technical potential of DHs to contribute to frequency containment reserves (FCR)	District heating	Review of EU countries
Gomez-Gonzalez M et al. [7]; 2019	Participation of specific technologies in FCR markets	Joint-optimization method for the sizing and power management of a household prosumer with photovoltaics (PV), EV charging, battery bank, household consumption, and power converters	Spain
Tukia T et al. [18]; 2018	Participation of specific technologies in FCR markets	Elevators/ MILP/ Stochastic model	The simulation was performed for each hour of the day for two-day types: weekdays and weekends
Uimonen S et al. [19]; 2019	Participation of specific technologies in FCR markets	3000 commercial and transportation escalators	Model Simulation
Fleer J et al. [20]; 2018	Participation of specific technologies in FCR markets	Battery energy storage system. The bidding strategies use a fundamental Primary control reserve price forecast model	The German model projection to the Great Britain
Melo S·P et al. [21]; 2018	Participation of specific technologies in FCR markets	Electric boiler with battery	Germany/A simulation model in MATLAB
Kaschub T et al. [22]; 2016	Participation of specific technologies in FCR markets	Stationary battery systems/Optimization model	Germany
Casals L.C et al. [23]; 2019	Participation of specific technologies in FCR markets	Reused electric vehicle batteries in buildings/ FRR market simulation	The public library near Barcelona (Spain)
Pandžić P et al. [24]; 2020	Participation of specific technologies in FCR markets	Battery storage as a price taker in the aFRR market /MILP by using the Karush–Kuhn–Tucker optimality conditions	Model for the European market based on the German market
Wang F et al. [25]; 2018	Participation of specific technologies in FCR markets	Combined heat and power facility with other technologies like photovoltaics with energy storage devices (electric and thermal)/ Optimization model	YALMIP toolbox in MATLAB
Posma J et al. [26]; 2019	Participation of specific technologies in FCR markets	Aggregated residential heat pumps/ Optimization model	Netherlands/The model has been developed in Python
Lesage-Landry A et al. [27]; 2020	Participation of specific technologies in FCR markets	Battery energy storage and water tank/Two-level algorithm for managing building energy consumption under uncertainty	Melbourne (Australia)
Astero P & Evens C [28]; 2020	Participation of specific technologies in FCR markets	Battery storages/ Optimized bidding strategy and online control methods of battery storage systems	Helsinki area (Finland)
Vannoni and Sorce [29]; 2024	Participation of specific technologies in the ancillary service market	A combined cycle gas turbine/MILP formulation and a machine-learning algorithm	Montecarlo approach based on historical data
Cremoncini D et al. [30], 2024	Participation of specific technologies in FCR markets	Hybrid battery energy storage system in a combination of lithium-ion (Li-ion) and vanadium redox flow batteries (VRFB) with participation in automatic frequency restoration reserve (aFRR) markets/ MILP	Danish Power Market
Subramanya R et al. [31]; 2021	Participation of specific technologies in FCR markets	Virtual power plant for distributed energy resources	Northern European shopping center (Finland). *Not specified.*
Terreros O et al. [32]; 2020	Participation of specific technologies in FCR markets	Heat Pumps in District Heating	Australia/ the state-of-the-art and future

(*continued on next page*)

Table 1 (*continued*)

Reference / Year	Objective	The area of use and Methodology or/and Model	Location or Environment or Study Type
			scenarios based on assumtions
Tan J et al. [33]; 2022	District heating system that acts as a prosumer participating in reserve markets	District heating system /An LP/MILP model	Bi-level model is reformulated into mathematical program with equilibrium constraints (MPEC) based on Karush-Kuhn-Tucker (KKT) conditions
Javanshir N et al. [34]; 2023	The operation of a District Heating Network in multiple energy markets, covering the day-ahead and intraday electricity markets, and various balancing markets	District heating networks (DHNs) equipped with power-to-heat (P2H) technologies and thermal storage	Finland
Iov F et al. [35]; 2020	The participation of power-to-heat (P2H) units in the ancillary service markets	Smart Grid Architecture Model (SGAM)	Denmark/A real-time control hardware-in-the-loop laboratory environment
Lotfi et al. [36]; 2024	The aggregator's income maximizing from vehicle-to-grid by contributing to the ancillary services markets	The robust OCC model, a robust LP model (RLP), is simulated using the CPLEX solver in GAMS software	The Electric Reliability Council of Texas (United States)
Wang and Hou [37]; 2024	Day-ahead bidding and real-time scheduling strategies for battery swapping stations to participate in frequency regulation	Electric vehicle battery swapping stations (BSS)/ information-gap decision theory (IGDT)	Pennsylvania, Jersey, and Maryland (United States)
Seo M et al. [38]; 2024	Electric vehicle bidding in the German frequency containment and restoration reserves market	Electric vehicle	Germany
Einolander J et al. [39]; 2023	Using electric vehicles (EVs) in household or explicit demand response settings	MILP model	Real-world data (Finnish company)
Einolander J & Lahdelma R [40]; 2021	Using electric vehicles (EVs) in household or explicit demand response settings	Multivariate copulas: the Gaussian (Normal) and Student-t copulas from the elliptical copula family; and Clayton, Frank, and Gumbel copulas from the Archimedean copula family	Real-life data (Finnish company) and through comparison with a previous non-copula application for EV FCR profile estimation
Astero P & Evens C [41]; 2021	Using electric vehicles (EVs) in household or explicit demand response settings	EVs are used as conventional power storage when connected to a home charge	Empirical charging data of public electrical vehicle charging stations in Helsinki (Finland)
Einolander et al. [42]; 2021	Using electric vehicles (EVs) in household or explicit demand response settings	EV battery to the grid (V2G); EV to the household (VTH)	Real-world data (Finnish company)
Einolander et al. [43]; 2022	Using electric vehicles (EVs) in household or explicit demand response settings	Individual charging events based on technical requirements of the frequency containment reserve for disturbance situations (FCR—D) /Deterministic model	Real-world data (Finnish company)
Utama C et al. [44]; 2020	Participation of specific loads in buildings in the electricity market through demand-side bidding	Air-conditioning loads in buildings	Singapore's Downtown Core/ The Python script
Stanislow L et al. [45]; 2024	Building stock model to an electricity system model	Based on the building model city-scale load curve creation in EnergyPlus	Simulation / Regina (the capital city of the Canadian province of Saskatchewan)
Korkas et al. [46]; 2022	Nearly optimal demand side management for controllable electric vehicles and energy storage systems for energy efficient operation of grid-connected buildings	Thermostatically controllable EV loads simulated and modelled in Energy Plus	*Not specified*

networks with power-to-heat (P2H) technologies [34] and thermal storage [35] were investigated. Smart Grid Architecture Models (SGAM) for market participation and reviews of business models for building participation in FCR markets [45] were included. Strategies for vehicle-to-grid (V2G) aggregators [36,42], battery swapping stations [37], electric vehicle bidding [38], and using EVs in household demand response settings [39–43] were also studied. Finally, nearly optimal demand-side management for controllable electric vehicles and energy storage systems in grid-connected buildings was proposed [45,46].

These studies provide insights into optimizing and managing various energy technologies and loads for effective participation in FCR and other ancillary service markets across different environments and settings.

None of the earlier studies have considered the overall optimization of sizing and operation of the hybrid energy system of a building including power and heat storages and participation in the FCR market. This signifies a considerable research gap. Additionally, the cost efficiency of power storage in buildings together with the FCR trade has not been assessed in previous studies. This study's novelty is optimizing energy solutions for buildings with a hybrid energy system that includes several energy technologies commonly used in Finland and that participate in the daily FCR-N market. Based on a model for optimal sizing and operation of building energy supplies and storages we determine the hourly FCR-N potential. Then we developed a novel LP model with hourly time resolution to simulate optimal FCR-N operation. The methodology is used to evaluate the cost-efficiency of FCR-N trade with different building energy system configurations. The LP model is an extension of a previous LP/MILP model for optimizing the configuration, sizing, and operation of a building energy system without FCR trade [47,48]. The previous study showed that in Finland district heating (DH) can work cost-efficiently in synergy with a ground source heat pump (HP) and this combination benefits significantly from heat storage (HS), but investment in power storage (PS) is far from cost-efficient. Another goal of the current study is to evaluate if FCR-N trade can make a PS cost-efficient for the target building. Overall, this study aims to bridge the research gap of previous studies while providing actionable insights to industry stakeholders about the cost-efficiency of different building energy system configurations and explicit demand response operation. This paper is structured as follows. In Section 2 we present the target building and the input data. In Section 3 we describe the methodology developed and applied in this study. In Section 4 we present the results on four configurations of the building energy system. Section 5 describes model validation. Section 6 contains conclusions and suggest directions for future research.

2. Case description

2.1. The target building

The target is an existing office building located in Helsinki, Finland. Currently, the building is heated by DH, and the HVAC systems have been designed to maintain good thermal comfort according to the building code. In this study, we consider retrofitting the building to include ground source HP, HS, and optional PS. HP is variable speed with an inverter drive unit allowing intake power to be adjusted freely [49]. The HS is a large insulated hot water tank, and the PS is a lithium-ion battery due to its fast response; thus, is more suitable for short-term storage and regulation [50]. Table 2 summarizes building properties.

Fig. 1 presents the hourly heating and power demand of the target building for the year 2020. Heat demand is low in the summer period, and shows typical variation depending on outdoor temperature, time of the day, and day of the week. Power demand is more stable throughout the year but with significant daily and weekly variations according to office hours.

2.2. Hybrid energy system of the target building

Fig. 2 illustrates the hybrid energy system for the building. The heat balance combines DH and HP heat sources with building heat demand and charge & discharge of the HS. The power balance combines PP from the grid with power consumption of the ground source HP, power demand for the rest of the building, and charge & discharge of an optional PS. This implements the *energy community* model, where all power demand is pooled together [47,51]. The energy community model is beneficial for FCR-N trade because it gives more flexibility to regulate power consumption when FCR-N capacity is activated.

Table 2
General target building data (heating and power data in 2020).

Office building	General data
Location	Helsinki
Gross area	22,771 m^2
Net area	18,522 m^2
Annual average heating demand	1354 MWh
Annual average power demand	1159 MWh

2.3. Input data

Table 3 presents cost information for this study. All prices include 24 % value added tax (VAT). Fixed costs for local technologies consist of investment costs per capacity (€/MW for HP, €/MWh for HS and PS) as an annuity with a 4 % interest rate and lifetime specific for each technology. The PS costs and other parameters are based on Tesla Powerpack [52]. Fixed costs for energy supply contracts (DH, PP) are the annual contract fees per capacity (€/MW). DH costs were calculated from the pricelist of Helen Ltd., which is the energy company of Helsinki. Power purchase from the grid (PP) has three price components, yearly constant fee (€), yearly capacity fee (€/MW), and energy fee (€/MWh). The energy fee is the Nord Pool hourly Elspot price plus electricity tax (22.53 €/MWh), distribution fee (32.8 €/MWh), and distributor margin (2.4 €/MWh) [53].

2.4. Power grid stability and FCR

FCR aims to keep the frequency of the power grid at the nominal 50 Hz frequency by regulating various power reserves up or down. Up-regulation means increasing power production or decreasing consumption to increase the grid frequency. Similarly, down-regulation means decreasing power production or increasing consumption to lower the frequency.

FCR is divided into two instruments, FCR-N for 'Normal' operation and FCR-D for more severe 'Disturbances'. FCR-N is a symmetrical product for both up- and down-regulation. This means that the provider of FCR-N resources must offer equal capacity for up- and down-regulation. FCR-N is the first response to frequency disturbances, and it is activated gradually when the frequency falls below 49.99 Hz or rises above 50.01 Hz. Fig. 3 shows the control curve for activation of FCR-N as a function of grid frequency. FCR-N resources are fully activated when the frequency falls below 49.9 Hz or rises above 50.1 Hz. The FCR-D resources activate in more extreme frequency disturbance situations after full activation of FCR-N [4].

In Finland, different reserve units such as power plants, consumption resources and energy storages, can participate on Fingrid's FCR-N market if they comply with the technical requirements, and pass the prequalification process described in [58]. In this process, system step response to ±0.1 Hz frequency deviations are measured. Full activation must be observed within 3 min of the simulated signal. Also, requirements for linearity of activation are defined. During operation, the FCR-N provider records actualized regulation with a time resolution less than or equal to 1 s and with a time stamp that should be synchronized to CET or UTC with high accuracy.

The pilot projects (2016–2020) described in [16] tried different business models to participate in the FCR market with building energy system technologies. Earlier pilots by Fingrid include using industrial freezers [59], residential electric space heating, hypermarket loads, and reserve generators in FCR. Currently all similar loads and load aggregators can participate on Fingrid's FCR marketplaces [60].

Fingrid acquires FCR-N resources from yearly and daily FCR-N markets based on bids from different actors. To acquire necessary hourly FCR-N capacity, Fingrid accepts bids in price-order, and all accepted bids are paid the price of the highest accepted bid for the hour (c_t^{FCR}). Bidding on the yearly market is done at the end of the previous year. Bidding on the daily market is done in the evening of the previous day by 18:30, and the accepted bids will be confirmed by 22:00 [61]. The bids must be made at 0.1 MW increments, and 0.1 MW is also the minimum bid size. However, several small actors can be aggregated together to reach the minimum bid size and increment.

In this study, we consider a building participating on the daily FCR-N market, and assume that bids are aggregated, allowing us to disregard

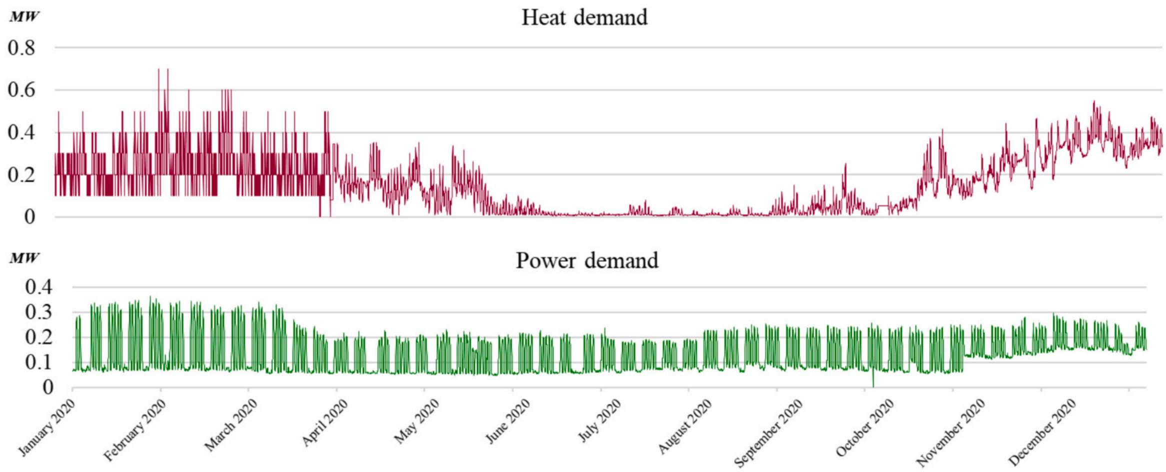

Fig. 1. Hourly heat and power demand for the target building in the year 2020.

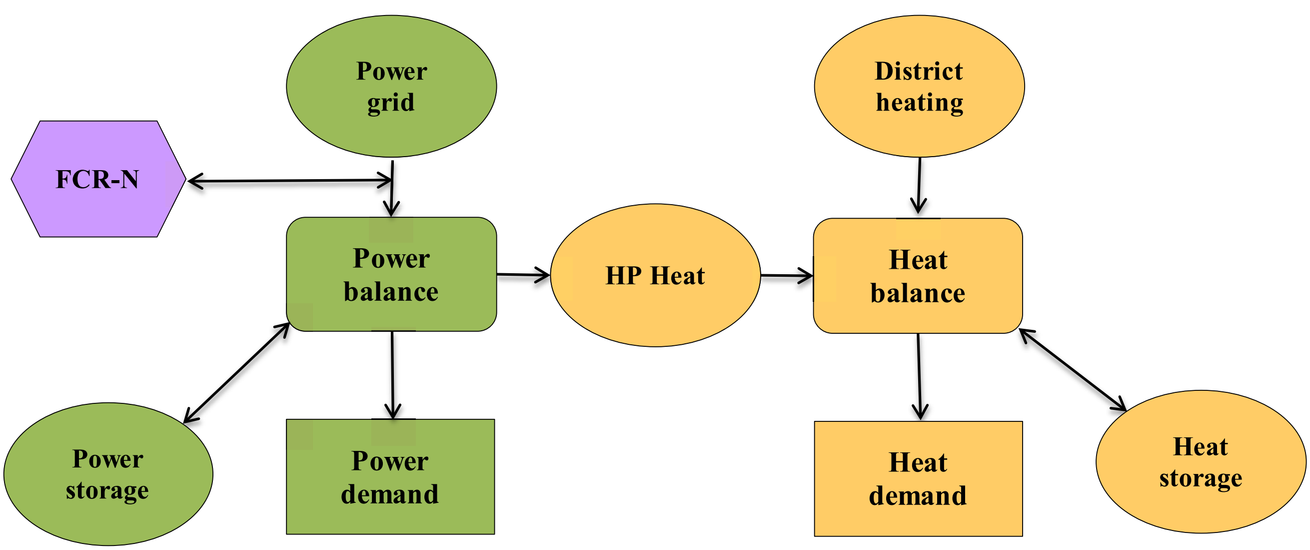

Fig. 2. Energy system for target building.

the 0.1 MW minimum bid and bid increment. Fig. 4 illustrates the FCR-N market in 2020. The first diagram shows the hourly market price on the daily market (€/MW), the second diagram shows the combined accepted bids from the yearly and daily markets (MW), and third diagram is the activated energy (MWh) for each hour. Average price on the 2020 daily FCR-N market was 21.19 €/MW, peak price was 160 €/MW, and lowest price was 1 €/MW. The activated energy is the hourly net activation where positive value indicates up-regulation and negative is down-regulation [60].

3. Methodology

The methodology for optimizing the building energy system with FCR-N consists of three phases:

1. Solve yearly planning model without FCR—N: The different energy solutions for the building are optimized without FCR. This is done using a yearly LP/MILP model that optimizes simultaneously the configuration, sizing, and operation of energy supply and storage units.
2. Estimate hourly FCR-N potential to make bids: For each day of the year a daily operative model is solved to determine optimal operation without FCR—N. Then, for each hour, the flexibility of the building to decrease or increase PP is analyzed to estimate the FCR-N potential for bidding on the daily FCR-market.
3. Daily operation with FCR-N activations: Daily operation of the building energy system with FCR-N is optimized for each hour of the day assuming maximal FCR-N bids.

In the following, we describe these phases in more detail.

3.1. Yearly planning model without FCR-N

The yearly planning model is an adaptation of the model presented in [47]. Based on historical or predicted hourly demand and price information, the model simultaneously solves the optimal configuration, sizing, and hourly operation of the building energy system by minimizing the combined fixed and operative costs. Yearly fixed costs for PP and DH contracts depend on corresponding capacity limits. Yearly fixed costs for HP, PS, and HS consist of investment costs per capacity as an annuity. The configuration (which technologies to include in the building) was in this study pre-set, i.e., there was no need to use MILP to optimize the configuration, and a pure LP model was enough. The adapted model is presented in Appendix A.

Table 3
Input data for the model.

Description / Capacity	Investment cost	Annuity factor (4 %)	Investment as annuity	Lifetime years	Reference
		Investment costs			
HP / 0.15 MW	1,300,000 €	0.090	116,923 €	15	[54]
HS/ 2.0 MWh	5376 €	0.074	396 €	20	[55]
PS / 0.1 MWh	385,000 €	0.123	47,467 €	10	[52]
		Annual costs			
DH capacity cost, €/MW	–	–	15,053	–	[56]
DH constant cost, €	–	–	2528	–	
DH price in 2020, €/MWh	65.92 1.1.-29.2.	62.19 1.3.-30.4.	34.87 1.5.-30.9.	63.62 1.10.-31.12.	
		Power market price			
Description	Average	Min	Max		Reference
Elspot price, €/MWh	28.02	−1.73	254.44	–	[57]

3.2. Hourly FCR-N potential and bidding

Hourly FCR-N potential is estimated one day at a time. First, an operative daily model without FCR-N is solved based on predicted heat and power demand, and power price. The operative daily model is obtained from the yearly planning model (Appendix A) by fixing the configuration and sizing of the building energy system and restricting the time horizon to 24 h. HS and PS storage levels at the beginning and end of the day are fixed half-full (or half-empty).

The FCR-N potential for each hour is then evaluated by calculating how much PP from the grid can be decreased in case of up-regulation or increased in case of down-regulation. Fig. 5 illustrates how the energy system can react to FCR-N activation by adjusting the HP or PS operation, or both, when necessary, but without affecting power consumption for the rest of the building. Adjusting HP operation will further affect the heat balance of the building, and this should be compensated by DH and HS. In practice, the DH contract is a little over-sized so that it can always compensate for a small amount of lacking heat. On the other hand, a small amount of excess heat will either fit in the heat storage or can be allowed to overheat the building for a short time without noticeable effect. Therefore, DH and HS are ignored when estimating the FCR-N potential.

The operative daily model determines for each hour t the optimal PP $x_{PP,t}$, HP operation $x_{HP,t}$, PS charge rate $s_{PS}^{IN,MAX}$, discharge rate $s_{PS}^{OUT,MAX}$, net charge rate $s_{PS,t}^{INOUT}$ (= charge rate minus discharge rate), storage level $s_{PS,t}$ and other variables. These quantities are used for estimating the hourly up- and down-regulation potential.

Up-regulation potential is computed as.

$$P_{UP,t}^{FCR} = min\left\{ x_{PP,t}, x_{HP,t} + min\left\{ s_{PS}^{OUT,MAX} + s_{PS,t}^{INOUT}, \eta_{PS}^{OUT}\left(s_{PS,t} - s_{PS,t}^{MIN}\right) / T_t^{FCR} \right\} \right\}. \quad (1)$$

Here, up-regulation potential cannot exceed $x_{PP,t}$ because PP cannot be negative. Otherwise, the up-regulation potential is the sum of the maximal decrease in HP power consumption ($= x_{PP,t}$) and maximal decrease in PS net charge rate. Decrease in net charge rate is constrained by maximal discharge rate $s_{PS}^{OUT,MAX}$. In addition, the minimum storage level $s_{PS,t}^{MIN}$ restricts the discharged energy to $s_{PS,t} - s_{PS,t}^{MIN}$. If the duration of full FCR-N activation is T_t^{FCR} (fraction of an hour), then maximal PS discharge is $\eta_{PS}^{OUT}\left(s_{PS,t} - s_{PS,t}^{MIN}\right) / T_t^{FCR}$ where η_{PS}^{OUT} is discharge efficiency. FCR-N providers with limited activation capacity must be capable of full activation for at least 30 min [58]. Limited activation capacity refers to storage-type units, that may become totally empty and therefore need time to recover their charge state. Therefore, we use the value $T_t^{FCR} = 0.5$ h here.

The down-regulation potential is not constrained by PP capacity, because the contract capacity limit x_{PP}^{MAX} is only monitored at an hourly level, while full FCR-N activation occurs for a fraction of the hour. Thus, down-regulation potential is computed by.

$$P_{DOWN,t}^{FCR} = x_{HP}^{MAX} - x_{HP,t} + min\left\{ s_{PS}^{IN,MAX} - s_{PS,t}^{INOUT}, \left(s_{PS,t}^{MAX} - s_{PS,t}\right) / \eta_{PS}^{IN} / T_t^{FCR} \right\}. \quad (2)$$

Here, the down-regulation potential is the sum of the maximal increase in HP power consumption ($= x_{HP}^{MAX}$-$x_{HP,t}$) and maximal increase in PS net charge rate. An increase in the PS net charge rate is constrained by the maximal charge rate $s_{PS}^{IN,MAX}$ and free storage capacity $s_{PS,t}^{MAX} - s_{PS,t}$ considering charge efficiency η_{PS}^{IN}.

As the power storage level is fixed half-full at the end of the daily model, only the heat pump contributes to the up and down-regulation potential for the last hour. This means omitting the PS-related terms in (1) and (2) for the last hour. Because up- and down-regulation capacity must be provided symmetrically in FCR-N trade, the FCR-N potential is

$$P_t^{FCR,BID} = min\left\{ P_{DOWN,t}^{FCR}, P_{UP,t}^{FCR} \right\} \cdot (1 - \sigma_t). \quad (3)$$

Because earlier FCR-N activations within the day affect a little the state (level of PS and HS) of the energy system for the remaining part of the day, earlier FCR-N activations may reduce the FCR-N potential for

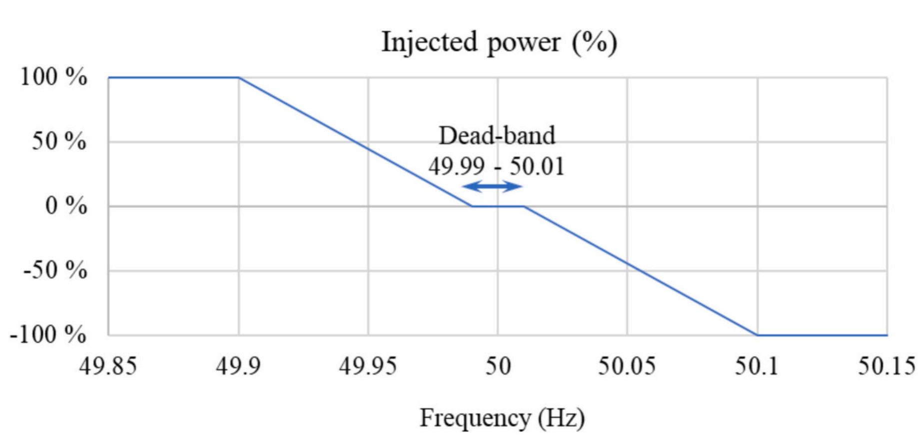

Fig. 3. The FCR-N activation as function of grid frequency.

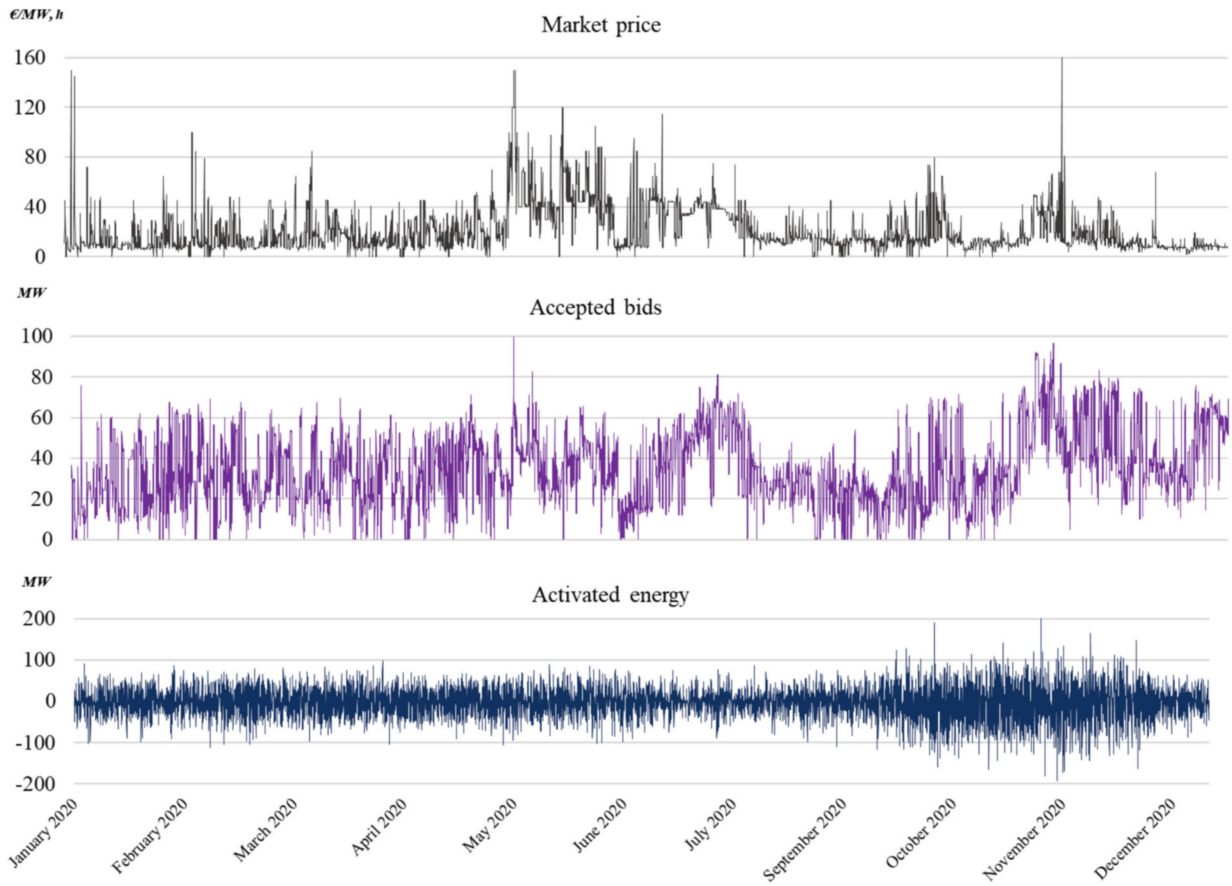

Fig. 4. Hourly FCR-N market price, accepted bids, and activated energy in the year 2020 [58].

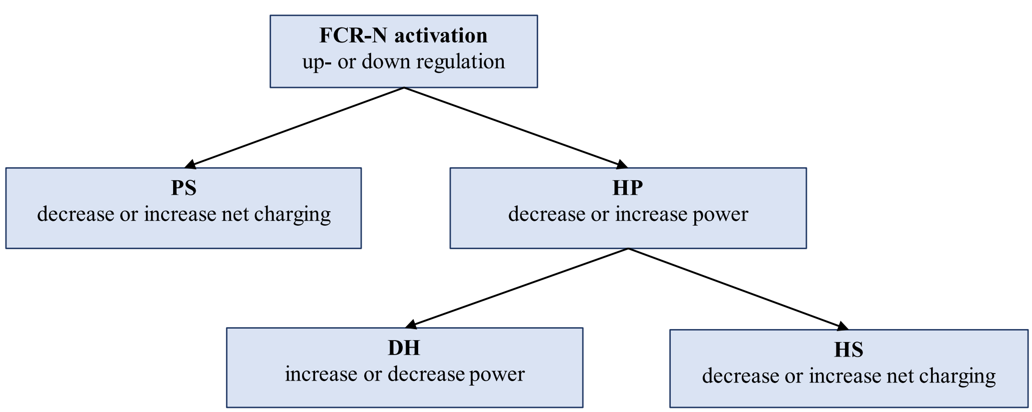

Fig. 5. Building energy system reaction to FCR-N activation.

subsequent hours. This cannot be considered in the FCR-N potential calculations because it is impossible to know beforehand the amounts and directions of FCR-N activations. Therefore, instead of bidding the estimated full FCR-N potential, we may decrease the bids a little by a *safety margin* σ_t that is zero for the first hour of the day but grows for subsequent hours. In this study we applied safety margins $\sigma_t = 1$ %·(t-1) for hours $t = 1, \ldots, 24$ of the day. We discuss the choice and effect of safety margin in the results section (4.6).

In addition to capacity (MW), the bids specify the bid price (€/MW). The bid price should be equal to or higher than the expected marginal operating cost increase of the energy system when adapting to an FCR-N activation. Simulation results show that this cost is in practice very low, and we can assume bids to be accepted for every hour.

3.3. Daily operation with FCR-N activation

FCR-N activation requires the building to adjust its power consumption. Up-regulation means that PP from the grid must decrease, and down-regulation means that PP must increase. Hourly activations are simulated based on Fingrid's history data for hourly activated net energy E_t^{FCR} (Fig. 4, third diagram). E_t^{FCR} is positive when up-regulation dominates, and negative for down-regulation.

Actual FCR-N activations occur on a minute- or a second level, but here we introduce a daily operational optimization model with FCR-N that approximates FCR-N activations on an hourly time resolution. Because up and down-activations are totally unpredictable before they occur, and follow a different time resolution than the daily operational optimization model, we develop a special modeling technique to extend the model with FCR—N.

Fig. 6 shows how minute-level activations are related to hourly activated net energy and illustrates the modeling principle. The top diagram shows minute level frequency for a sample hour and corresponding FCR-N activation that depends on how much the frequency deviates from 50 Hz. The middle diagram presents the same frequency and activation information sorted by activation. This illustrates the down-regulation energy as an area below the zero-level, zero activation in the dead-band [49.99 Hz, 50.01 Hz, Fig. 3] and up-regulation as the area above the zero-level. Up-regulation area minus down-regulation area is the activated net energy E_t^{FCR} for the hour. The bottom diagram illustrates how the FCR-N activation is represented in our model by a rectangular block with area E_t^{FCR}. The height of the rectangle is the accepted bid $P_t^{FCR,BID}$ (maximum FCR-N power) and width is the *utilization period of maximum FCR-N power*

$$T_t^{FCR} = E_t^{FCR} / P_t^{FCR,BID}. \tag{4}$$

Because $P_t^{FCR,BID}$ is non-negative, T_t^{FCR} has the same sign as E_t^{FCR} and is negative for down-regulation. The rectangular activation shape can be interpreted as the 'worst case' activation that is most difficult to react to, because it requests maximal regulation to be activated at the last moment within the hour. Therefore, if the building can respond to rectangular FCR-N activation, it can also respond to an arbitrary minute-level activation profile with the same net energy.

3.3.1. Constraints and decision variables

Next, we define the LP model for optimizing daily energy system operation with FCR—N. This model is an extension of the daily operative model with additional decision variables and constraints. The main decision variables are P_t^{FCR} for each hour denoting FCR-N activation power. Fixing each P_t^{FCR}=0 yields the operative daily model without FCR—N, while fixing $P_t^{FCR} = P_t^{FCR,BID}$ requests maximal activation for the hour. Thus, the same LP model can optimize daily operation with and without FCR-N trade only by adjusting the upper and lower bounds of certain variables.

The model must make sure that both the activated FCR-N power (MW) and energy (MWh) can be supplied during the hour. The activated power is represented as a sum of three non-negative decision variables that determine how the building energy system reacts to the activation:

$$P_t^{FCR} = P_t^{FCR,HP} + P_t^{FCR,PS} + P_t^{FCR,X}. \tag{5}$$

Here $P_t^{FCR,HP}$ is the change in HP power, $P_t^{FCR,PS}$ is change in PS net charge rate, and $P_t^{FCR,X}$ is unsupplied FCR-N capacity in case the requested activation exceeds the flexibility of the energy system. Bounds for the activation power variables are

$$P_t^{FCR} \geq 0, \tag{6}$$

$$0 \leq P_t^{FCR,HP} \leq min\{x_{HP,t}^*, x_{HP}^{MAX} - x_{HP,t}^*\}, \tag{7}$$

$$0 \leq P_t^{FCR,PS} \leq min\left\{s_{PS}^{IN,MAX} - s_{PS,t}^{INOUT,*}, s_{PS}^{OUT,MAX} + s_{PS,t}^{INOUT,*}\right\}, \tag{8}$$

$$P_t^{FCR,X} \geq 0. \tag{9}$$

The upper bound for HP regulation (7) is determined based on the maximal up- and down-regulation from current operating level $x_{HP,t}^*$ that

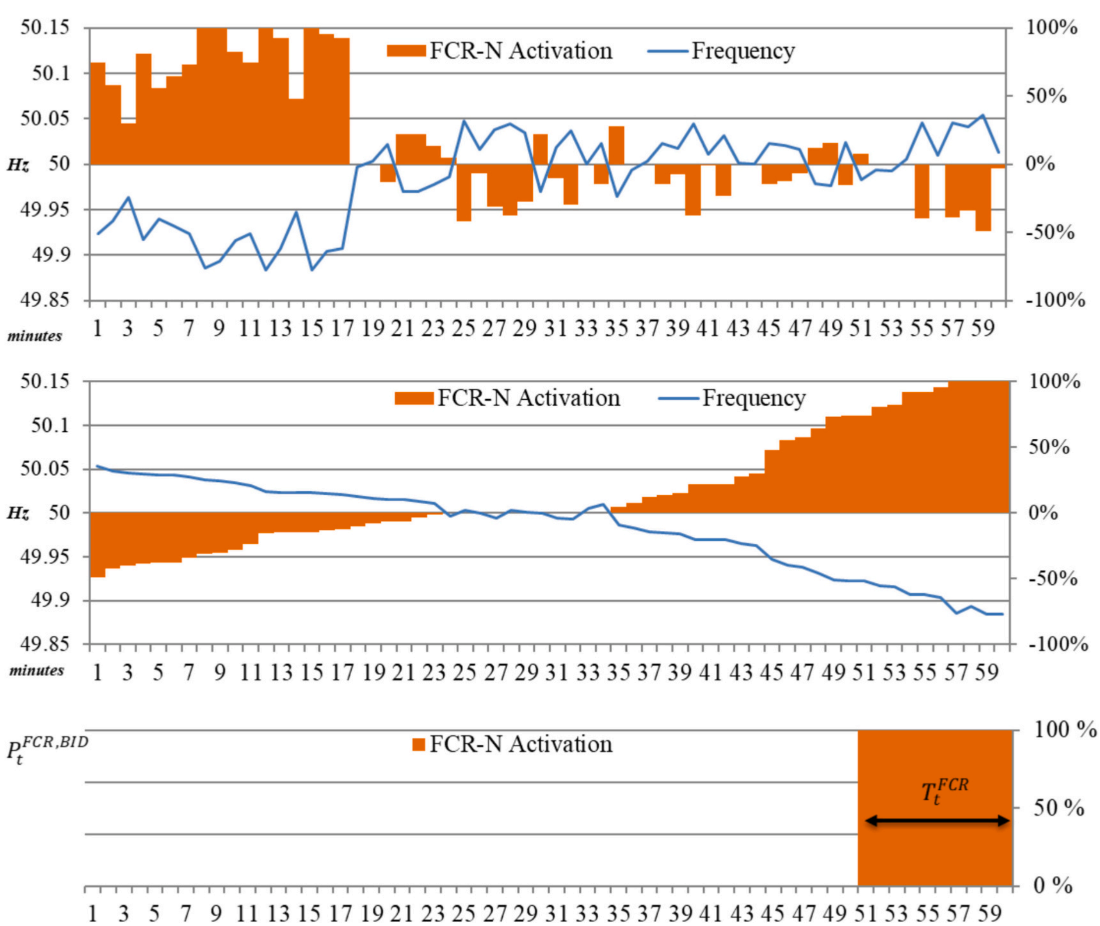

Fig. 6. Top diagram: Minute-level frequency and FCR-N activation for a sample hour; Middle diagram: Same information sorted by activation; Bottom diagram: Representing the net activation at hourly time resolution.

was obtained by solving the model without FCR—N. Similarly, upper bound for PS regulation (8) is based on maximal down- and up-regulation from current PS net charge rate $s_{PS,t}^{INOUT,*}$.

The optimized electric energy purchase $x_{PP,t}^{*}$ changes due to the FCR-N activation by $-T_t^{FCR}\left(P_t^{FCR,HP}+P_t^{FCR,PS}\right)$, i.e. PP decreases when $T_t^{FCR}>0$ and increases when $T_t^{FCR}<0$. For the HP the activation means that electrical energy for the HP changes from earlier optimized value $x_{HP,t}^{*}$ by $-T_t^{FCR}P_t^{FCR,HP}$. Similarly, for the PS, net charge rate changes by $-T_t^{FCR}P_t^{FCR,PS}$. Substituting these into the hourly power balance constraint (A.3), HP production constraint (A.4) and storage charge/discharge constraint (A.9) in Appendix we obtain

$$x_{PP,t}^{*}-T_t^{FCR}\left(P_t^{FCR,HP}+P_t^{FCR,PS}\right)-\left(x_{HP,t}-T_t^{FCR}P_t^{FCR,HP}\right)-\left(s_{P,t}^{INOUT,*}-T_t^{FCR}P_t^{FCR,PS}\right)=d_{P,t}, \tag{10}$$

$$x_{HP,t}^{H}=\eta_{HP,t}\left(x_{HP,t}^{*}-T_t^{FCR}P_t^{FCR,HP}\right), \tag{11}$$

$$s_{PS,t}^{INOUT,*}-T_t^{FCR}P_t^{FCR,PS}=s_{PS,t}^{IN}-s_{PS,t}^{OUT}. \tag{12}$$

Note that in (10) all FCR-terms cancel out, and the constraint becomes equivalent to the original energy balance constraint (A.3) with PP, HP, and PS variables fixed: $X_{PP,t}=x_{PP,t}^{*}$, $x_{HP,t}=x_{HP,t}^{*}$, $s_{PS,t}^{INOUT}=s_{PS,t}^{INOUT,*}$ Constraints (11) and (12) replace the original constraints (A.4) and (A.9). The heat side of the model will adapt automatically to FCR-N activation.

3.3.2. Objective function

FCR-N trade affects the revenues and operating costs in three ways:

- The activation of FCR-N diverts the building from optimal operation, which in general results in slightly higher operative costs for the overall time horizon. However, operating costs for individual hours can be higher or lower.
- FCR-N market price is paid for accepted bids. However, if the full amount of regulating capacity cannot be delivered, the revenue is cut by non-delivered capacity.
- A penalty fee must be paid for the non-delivered capacity part.

The profitability of FCR-N trade depends on whether the revenues from FCR-N trade exceed the increase in operative costs and possible penalty fees. The costs and revenues are considered by adding the following terms to hourly operating costs in (A.1):

$$C_t^{FCR}=-c_{PP,t}\,T_t^{FCR}\left(P_t^{FCR}-P_t^{FCR,X}\right)-c_t^{FCR}\left(P_t^{FCR}-P_t^{FCR,X}\right)+c_t^{FCR,X}P_t^{FCR,X}. \tag{13}$$

The first term is change in PP costs due to FCR-N regulation, second term is revenue from FCR-N trade, and third term is penalty for non-supplied capacity. $c_{PP,t}$ is hourly power price, c_t^{FCR} is the FCR-N market price, and $c_t^{FCR,X}$ is the penalty fee. Change in DH costs is automatically considered by the model. According to the FCR-N contract, the penalty fee is equal to c_t^{FCR}. However, FCR-N trade conditions allow delivery of less than full capacity only in forcing situations. Therefore, instead of applying the rather low penalty, the model applies a much higher penalty to restrict non-delivery to forcing situations.

3.3.3. Optimization of daily FCR-N operation

Initially, FCR-N capacity for each hour of the daily FCR-N model is fixed P_t^{FCR}=0 and optimized. (Fixing FCR-N capacity to zero makes the model equivalent to the daily model without FCR—N). Then, to optimize the FCR-N activation, the model was modified and solved iteratively in two steps for each hour $t=1,\ldots,24$:

- Decision variables for earlier hours 1, …, t-1 are fixed to previously optimized values, as FCR-N activation during hour t must not affect the past operation. The model is also modified by fixing the PP variable to the optimized *baseline* value $x_{PP,t}=x_{PP,t}^{*}$ and fixing FCR-N capacity to accepted bid power $P_t^{FCR}=P_t^{FCR,BID}$.
- The modified model is solved for the remaining hours t, …, 24 to optimize the FCR-N activation for hour t in terms $P_t^{FCR,HP}$, $P_t^{FCR,PS}$, and $P_t^{FCR,X}$ (5).

This method resembles the idea in the *sliding time window method*, where a longer time horizon model is solved to get optimal solution for a shorter time span [62]. This scheme is implemented using the LP2 linear and mixed integer programming software [63]. LP2 supports re-optimizing a model efficiently in-memory, while fixing variables to different values between optimizations. All optimization runs were performed in an efficient Windows PC.

4. Results and discussion

We present first results on sizing the building, then operating costs in different configurations, followed by details on power and heat side operation and storages, without and with FCR—N.

4.1. Sizing based on long-term planning model

To determine the optimal sizing of the PP and DH contracts, the HP, and storages HS & PS without FCR-N trade we solved the yearly planning model for the building based on heat and power demand data and Nord Pool Elspot power price for 2020. This resulted in the following sizing to be used in further analyses: PP: 0.5 MW, DH: 0.05 MW, HP: 0.15 MW, and HS: 2.0 MWh. The ground source HP operates by a constant COP factor of 3.5, whereby it can produce a maximum of 0.525 MW heat. The capacity limit for DH is quite low, because the HP together with a large HS can supply heat cheaply most part of the year.

In agreement with our earlier studies [47,48], a large HS was highly cost-efficient, but optimal size for PS was 0, i.e., PS was not cost-efficient without FCR-N trade. However, in the following analyses we also include configurations with a 0.1 MWh PS (one Tesla Powerpack unit), because we wanted to study if FCR-N trade can make the PS profitable. An interesting observation was that including a 0.1 MWh, or 0.2 MWh PS had practically no effect on optimal sizing of the other components. The fixed annual costs for the studied configurations are (based on Table 3) 24878 € without PS, 27286 € with 0.1 MWh PS and 32,033 € with 0.2 MWh PS.

4.2. Operating costs in different configurations

For FCR-N trade we applied maximal bids calculated as presented in 3.2. In the following, we analyze and compare the following four configurations:

1. Without PS, without FCR—N.
2. Without PS, with FCR—N.
3. With 0.1 MWh PS, without FCR—N.

Table 4
Annual operating costs in four configurations: without and with the PS; without and with FCR—N.

	Operating costs (€)			FCR-N Costs, Penalties, Revenue (€)		
Configuration	No FCR	With FCR	*Difference*	Costs	Penalties	Revenue
No PS	172 987	171 202	1785	357	19	−2161
PS 0.1 MWh	171 825	166 299	5527	363	55	−5945
Difference	1162	4904	6689	-6	-36	3784

4. With 0.1 MWh PS, with FCR—N.

Table 4 presents the optimized yearly operative costs in the four configurations and FCR-N costs, penalties, and revenue in the corresponding two configurations. Compared to the base case of without PS and FCR-N trade, FCR-N trade lowers the operative costs by 1785 €, while PS lowers the costs by 1162 €. The combined benefit from FCR-N and PS is 6689 €. Because the combined benefit is much larger than the sum of separate benefits, this indicates clear synergy between PS and FCR-N trade.

To assess the cost-efficiency of the PS, savings in operating costs must be compared with the investment costs as annuity, which according to Table 3 is 47,467 €/MWh, i.e., 4747 € for the 0.1 MWh PS. This means that the PS is not cost-efficient without FCR-N trade. With FCR-N trade the PS lowers the annual operating costs by 4904 €, which makes the PS (slightly) profitable.

FCR trade reduces the operating costs by 1785€ (1.0 %) without PS and by 5527€ (3.2 %) with 0.1 MWh PS. The profitability of FCR-N trade originates from the direct revenues of FCR-trade. The additional yearly PP&DH energy costs are small, 357 € and 363 €, and penalties for

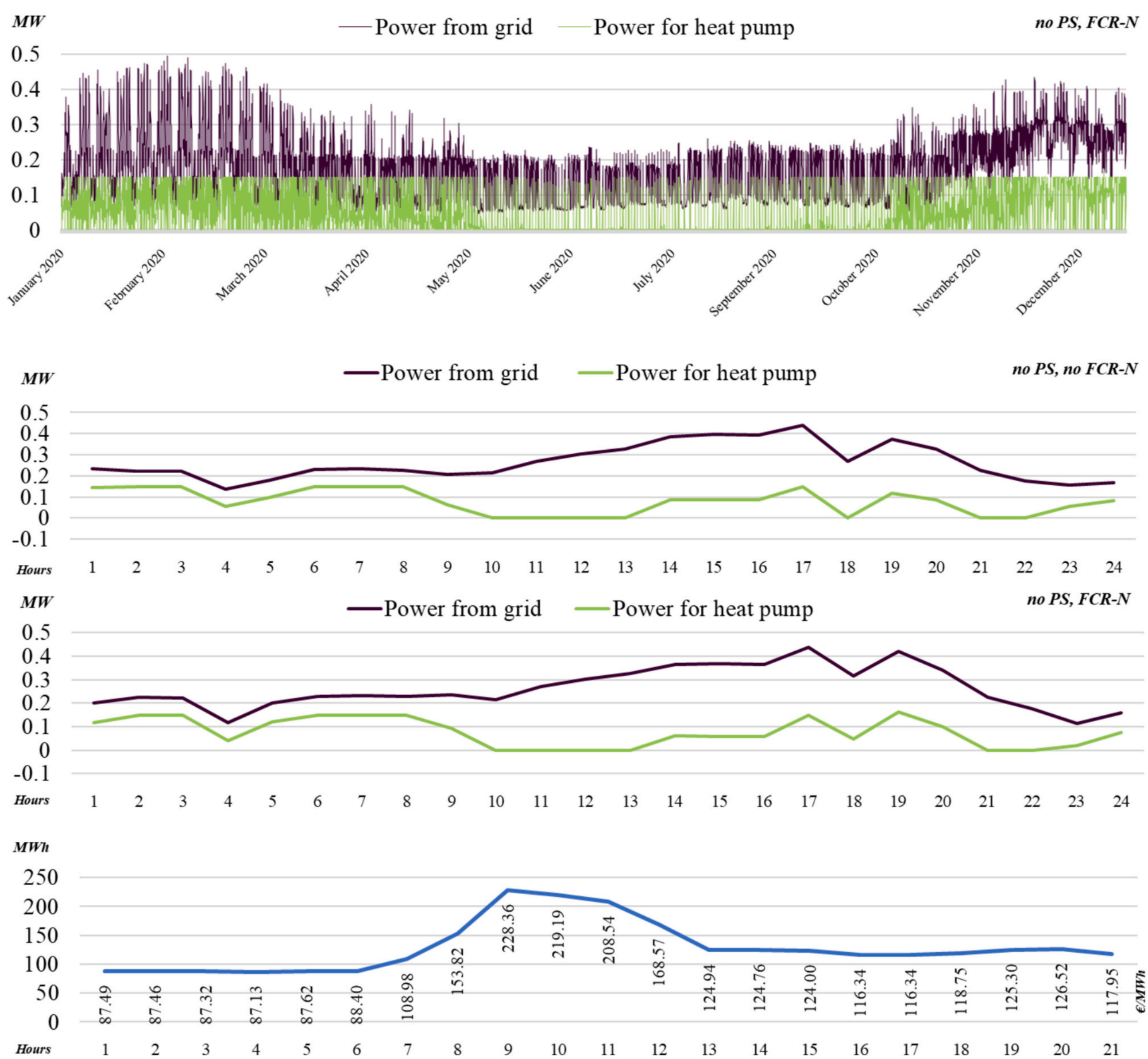

Fig. 7. Results without PS – Power side operation. Diagram 1 shows yearly data without FCR-N.
Diagrams 2 and 3 illustrate results without and with FCR-N for a single day (May 18, 2020).

unsupplied capacity are minimal, 19 € vs 55 € without and with PS, correspondingly. Total yearly unsupplied FCR-N capacity was 1.9 MW (out of 124 MW) vs 5.0 MW (out of 302 MW) without and with PS. Because the hourly model approximates maximal hourly activation conservatively, in reality the unsupplied capacity and penalties should be even smaller.

4.3. Results on power side operation

Fig. 7 presents results without a PS on PP and HP power. The first diagram presents the results without FCR-N for the full year. The full year diagram with FCR-N is omitted because it looks almost identical. The second and third diagram illustrate the operation without and with FCR-N for a single day (May 18, 2020). The fourth diagram shows the power price for the same day. Due to implicit demand response, the heat pump does not operate during most of the day-time when power price is high. While there are minor differences in PP and HP operation, in general FCR-N affects building operation very little. Yearly PP for the HP with FCR-N (414 MWh) is only 2 MWh smaller than without FCR-N trade (416 MWh).

Fig. 8 presents results with PS on PP, HP power, and net charge of the PS. Again, the first diagram presents the results without FCR-N for the full year and the second and third diagrams illustrate the differences without and with FCR-N for a single day. Implicit demand response shuts again off the HP for most of the day-time due to high power price, and the HS is discharged instead (see next section). The daily profiles of PP and HP utilization are now quite different from the no PS cases due to optimal charging and discharging of the PS. FCR-N activations make PP use smoother while PS is charged and discharged more aggressively to respond to changes in HP operation. The number of yearly full charge/discharge cycles for the PS is 386 without FCR-N and 473 with FCR—N. The main effect of the PS is that it increases the FCR-N potential significantly, resulting in larger activations. The FCR-N potential added over the year is 302 MW with PS compared to 124 MW without PS.

The FCR-N activation for one hour may reduce the FCR-N capacity for subsequent hours, and thus result in unsupplied activation power $P_t^{FCR,X}$ in (5), but this occurs rarely. One reason is that up-regulations and down-regulations mostly cancel out within some hours. Secondly, the 30 min recovery time for limited activation capacity resources allows the building to recover at least partly its planned flexibility for subsequent activations.

The results show that requested FCR-N activation can be supplied with high probability during the year in various operating situations. Based on the load duration curve with PS for the full year (Fig. 9), the unsupplied activation power is maximally 0.1 MW, a totally 5 MW during the year, and it occurs only during 4 % of the hours (380 h / 8784 h).

In real life, the unsupplied activation power should be even lower, because the model approximates the FCR-N conservatively, the DH contract provides in practice extra sub-hour flexibility for up-regulation, and it is also possible to increase flexibility for down-regulation occasionally by over-heating the building a little without compromising thermal comfort.

4.4. Results on heat side operation

Fig. 10 presents results without a PS in terms of HP heat production, DH purchase and net charge of the HS. When the HP reacts to FCR-N

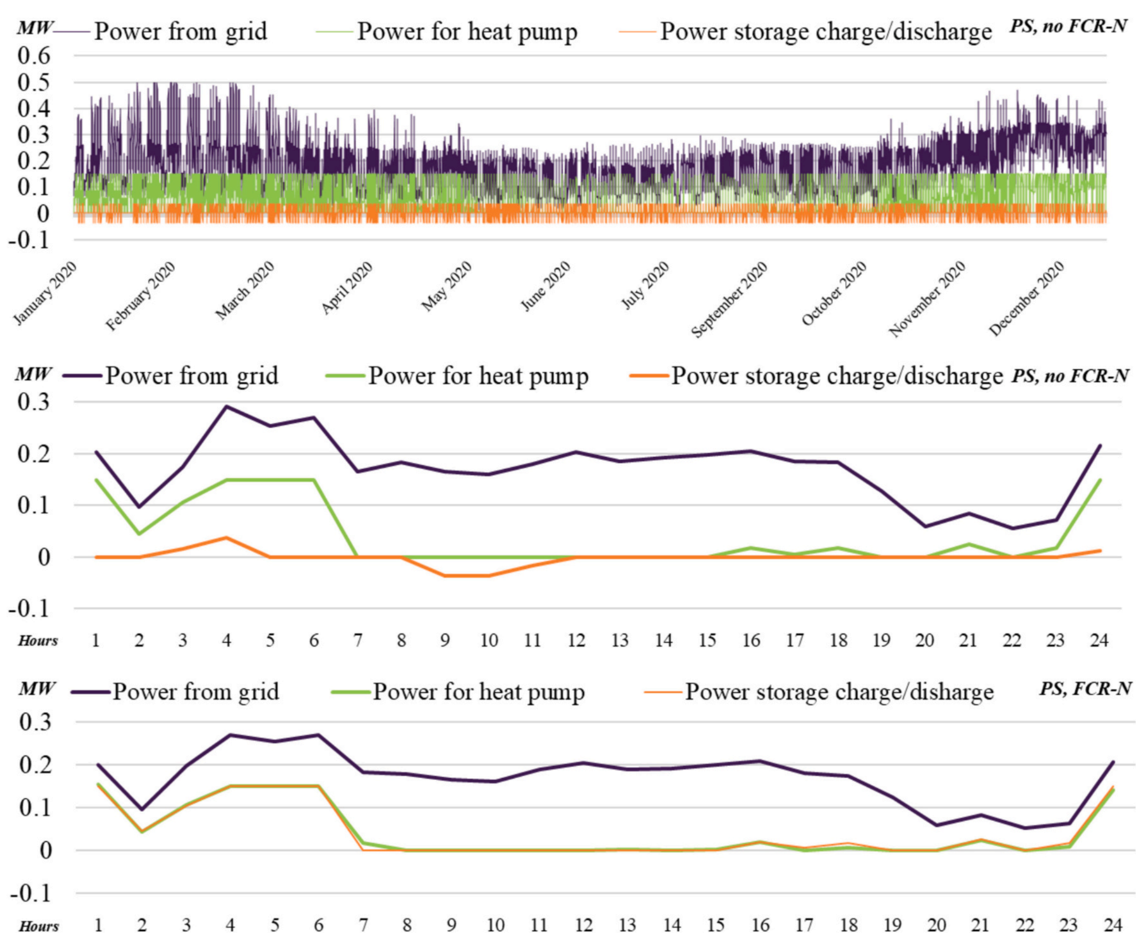

Fig. 8. Results with PS – Power side operation. Diagram 1 shows yearly data without FCR-N. Diagrams 2 and 3 illustrate results without and with FCR-N for a single day (May 18, 2020).

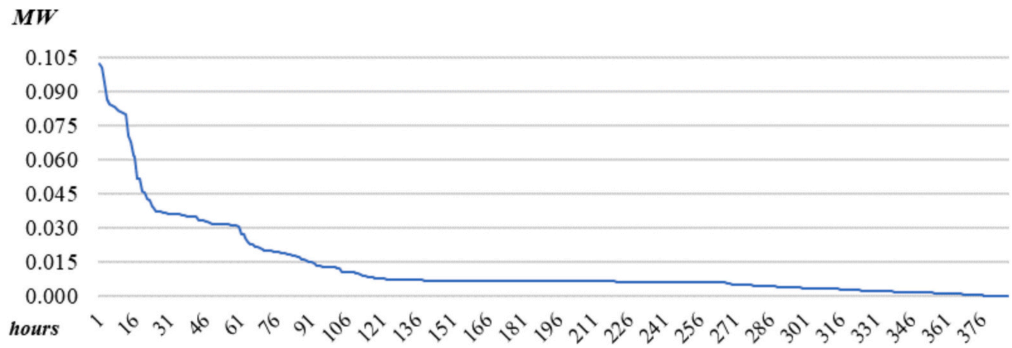

Fig. 9. Results with PS – Load duration curve for unsupplied FCR-N power ($P_t^{FCR,X}$).

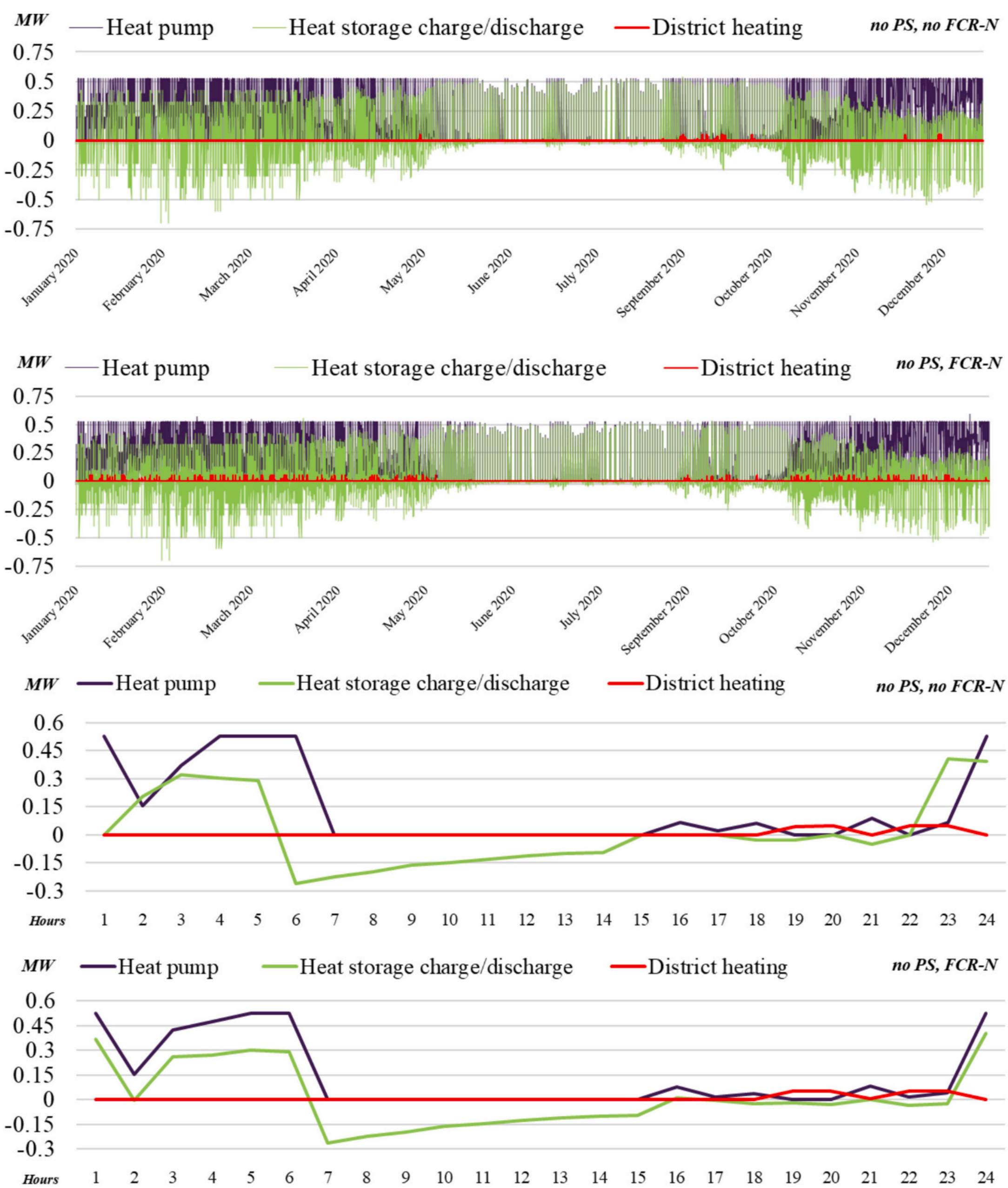

Fig. 10. Results without PS – Heat side operation. Diagrams 1 and 2 show yearly data without and with FCR—N. Diagrams 3 and 4 illustrate results without and with FCR-N for a single day (May 18, 2020).

activation, that leads to adjusting heat side operation (Fig. 5). Overall, FCR-N does not affect much the heat side operation. Comparison of the yearly diagrams (first two) without and with FCR-N show that with FCR-N the DH purchase is much more volatile during most of the year except in the summer when no DH is used. Also, the yearly DH purchase with FCR-N (10 MWh) is much larger than without (2.7 MWh). This means that although DH capacity is quite low, it still contributes significantly to the flexibility of the energy system to serve FCR—N. HP operation varies actively between minimal and maximal (0.525 MW) heat production in both configurations. The HS is charged with heat from the HP during the early morning when the power price is low and discharged in day-time when the power price is high.

Fig. 11 presents results with PS in terms of HP heat production, DH purchase, and net charge of the HS. Again, the yearly diagrams (first two) show that DH purchase is much more volatile with FCR-N than without. Also, the yearly DH purchase with FCR-N (6 MWh) is larger than without (2.7 MWh), but not as large as it was in the configuration with FCR-N but without PS. Thus, the PS has significantly reduced the burden of DH to adapt to FCR—N.

The daily diagrams show small changes in HS operation due to FCR—N. The yearly utilization of the HS is 200 charge/discharge cycles without FCR-N (both without and with PS). With FCR-N HS utilization is 208 with PS and 215 cycles without PS.

4.5. Sensitivity analysis

Many of the results depend on factors that are uncertain, imprecise, subject to change, or dependent on local conditions. Future case studies should apply recent locally applicable estimates for such factors.

Normally fairly accurate estimates for costs and technical parameters should be available for the energy technologies when planning the investment. Such factors affect the optimal configuration and dimensioning but do not affect the operation and operational costs. Other factors, such as the level of power price, DH price, and FCR-N capacity price will vary during system lifetime and will affect the optimal operation and operational costs. We apply sensitivity analysis to evaluate

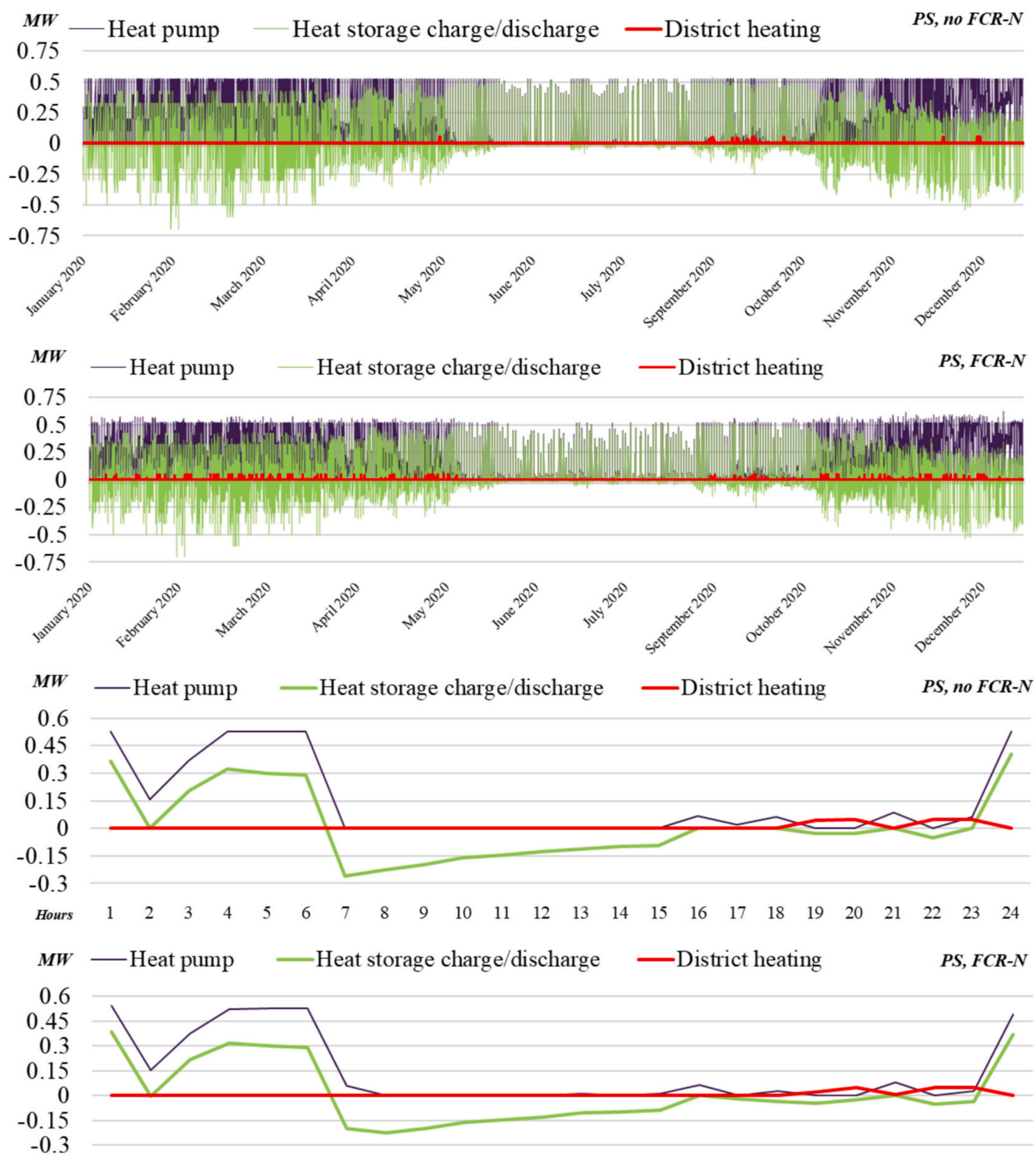

Fig. 11. Results with PS – Heat side operation. Diagrams 1 and 2 show yearly data without and with FCR—N. Diagrams 3 and 4 illustrate results without and with FCR-N for a single day (May 18, 2020).

Table 5
Sensitivity analysis on PP price, DH price, and FCR-N with respect to base cases 2&4.

	Operating costs (€)			FCR-N Costs, Penalties, Revenue (€)		
Configuration	No FCR	With FCR	*Difference*	Costs	Penalties	Revenue
Base cases 2&4	171 825	166 299	5 527	363	55	5 944
PP price +10 %	188 985	183 472	5 513	359	56	5 929
PP price −10 %	154 650	149 120	5 531	364	55	5 950
DH price +10 %	171 833	166 331	5 502	392	56	5 950
DH price −10 %	171 801	166 252	5 549	323	56	5 929
FCR-N price +10 %	171 825	165 710	6 115	363	61	6 539
FCR-N price −10 %	171 825	166 887	4 938	363	50	5 350

their impact on optimal operation.

Table 5 presents how optimal operation changes subject to 10 % increase and decrease in PP price ($c_{P,t}$), DH price ($c_{H,t}$), and FCR-N (c_t^{FCR}) price. As base cases, we use configurations 2&4 (Section 4.1) with 0.1 MWh PS, without and with FCR-N trade. Increasing the power price by 10 % leads to a little reduced HP operation and, to compensate, higher DH consumption. Overall operating costs have increased slightly >10 %. The effect on FCR operation and revenue from FCR trade is minimal (−14€). Lower power price has similar but opposite effects. Increasing the DH price by 10 % leads to lower DH consumption and slightly higher HP operation. Overall operating costs increase only by 0.02 % because DH is responsible for a small fraction of heat acquisition. Again, the effect on FCR operation and revenue from FCR trade is minimal. Lower DH price has similar but opposite effects. Increasing the FCR-N price by 10 % affects only the FCR revenue and penalties increasing them by 10 %. Otherwise, the operation of the system remains unchanged. We conclude that the profitability of the FCR-N trade is very robust with respect to changes in power and DH price, but directly affected by the price level on the FCR-N market.

Because the presented methodology initially optimizes the sizing of the hybrid energy system without FCR—N, it does not necessarily lead to global optimum with FCR—N. The main purpose of the energy system is to satisfy the heat and power demand in all operative situations economically, while FCR-N trade has a lesser effect on energy system operation and economy. Therefore, the dimensioning without FCR-N is a good starting point for seeking the optimum with FCR—N. We have performed sensitivity analysis in terms of sizing HP, HS, and PS. Sensitivity analysis shows that increasing:

- HP capacity from 0.15 MW to 0.02 MW increases total annual costs by 1793 €
- HS capacity from 2.0 MWh to 0.2 MWh increases total annual costs by 284 €
- PS capacity from 0.1 MWh to 0.1 MWh increases total annual costs by 564 €.

This indicates that the obtained solution is at least a local optimum.

4.6. Discussion

Technological advancement and growing markets can be expected to reduce investment costs and improve the efficiency of novel energy technologies in the future, but energy prices for heat and power are more likely to increase than to decrease. Such development should favor novel and more complicated hybrid energy systems for buildings.

Based on sensitivity analysis, the profitability of FCR-N trade depends most significantly on the price level of the FCR-N market. It is hard to predict what will happen in the FCR-N market. Increasing amounts of intermittent renewable power will increase the demand for various reserves and tend to raise the price level but increasing the supply of capacity by various actors has the opposite effect on the FCR-N price.

The slight profitability of PS together with FCR-N is strongly dependent on PS investment costs and lifetime. The lifetime of the PS can possibly be extended beyond the warranty period, or the battery can alternatively be sold for some residual value on the second-life battery market [64].

The purpose of the safety margins σ_t in (3) is to reduce the probability of unsupplied activation power. Choice of σ_t is not a pure economic optimization problem, because the spirit of the FCR-N contract is to allow non-supply only in forcing situations. The results were computed by applying $\sigma_t = 1$ %·(t-1) for hours $t = 1, \ldots, 24$ of each day. Fig. 12 shows the effect of the safety margin on unsupplied FCR-N capacity and operating costs with PS. Doubling σ_t reduces unsupplied FCR-N power from 5 MW to 4 MW, but also increases yearly operating costs by 590 € due to smaller revenue from FCR-N bidding. Setting σ_t to zero, increases unsupplied FCR-N capacity to 6.7 MW, but reduces operating costs by 580 €. The ideal values for the safety margins need to be adjusted based on real-life operation.

5. Model validation

The planning model without FCR-N has been validated for different time horizons and different configurations of energy supplies and storages in connection to earlier studies by constructing the model incrementally and validating each component first separately and then together [47,48]. Also, the model has been tested on multiple buildings of different types. Additional validation is needed for the method for estimating FCR-N bidding potential and for the daily operative FCR-N model developed in this study.

The daily FCR-N model was developed as an extension of the model without FCR—N. Validation of the FCR-N model involved several steps. First, with zero-size bids the FCR-N model was validated to be equivalent to the model without FCR—N. This was confirmed both theoretically by analyzing the model structure and experimentally by ensuring that the FCR-N model gave identical results to the model without FCR—N. Secondly, the FCR-N model was tested with different size FCR-N bids against actual history data to see that the results were feasible. The FCR-N model approximates at hourly level the reaction to sub-

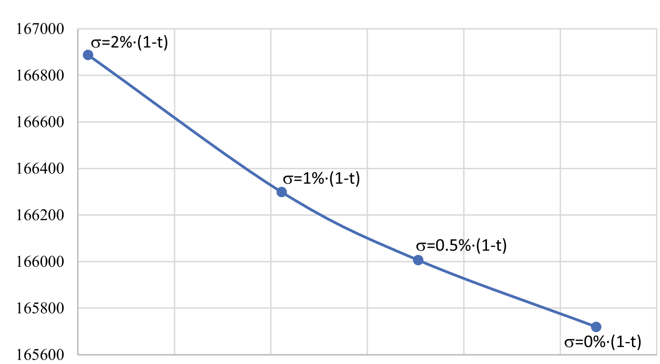

Fig. 12. Effect of safety margin (σ) on unsupplied FCR-N capacity and operating costs with PS.

hourly activation of FCR—N. Therefore, the hourly results of the model were compared against minute-level historical data on grid frequency and resulting FCR-N activations to validate that the system responds to the actual activation requests properly. The optimality of the hourly demand response was confirmed by verifying that the different flexibility mechanisms (PS, HP, HS, DH, see Fig. 5) were employed in merit-order depending on the current operating situation. Thirdly, the entire daily model was validated by simulating operation over the days of a full year. This involved verifying that the cumulative effect of subsequent up- or down-activations affects the state of storages (PS, HS) properly, resulting sometimes in reduced flexibility for future hours. The inability to respond to FCR-N activation was correctly observed as a positive value for the variable $P_t^{FCR,X}$.

Estimation of maximal FCR-N bidding potential was validated to lead to feasible models for individual hours. However, to consider the reduced flexibility due to the cumulative effects of previous activations on storages, a heuristic approach using safety margins (σ_t) to reduce the bids was introduced. Sensitivity analysis was used to verify that unsupplied FCR-N capacity decreased monotonically and (net) operating costs increased monotonically when σ_t was increased. See Fig. 12 for the effect of the safety margin on the model with PS.

6. Conclusions and future research

We have developed a new methodology for optimizing the explicit demand response trade in the daily FCR-N market and operation of a building with a hybrid energy system that includes DH and PP contracts, ground source HP, and storages for heat and power (HS, PS).

Optimal FCR-N operation is simulated by a novel LP model on hourly time resolution. Testing the model on a sample building showed that FCR-N trade is profitable, and PS can be cost-efficient together with FCR-N trade. The methodology is general and extends easily to other building energy solutions. FCR-N trade has proven to be profitable for building with a hybrid energy system. For example, a specific building experienced an annual benefit of €5527 from FCR trade, equating to approximately a 3 % reduction in annual operating costs. This decrease, though seemingly modest, can improve the financial situation of the building's owner or operating company, providing a tangible economic advantage and enhancing overall operational efficiency.

The current study applied a deterministic technique to estimate FCR-N bidding potential. Further research on more advanced stochastic bidding techniques could use the presented LP model to test and compare them. While the current model approximates the FCR-N activations conservatively using hourly time resolution, actual FCR-N regulation must occur in seconds or minutes. It would be interesting to adapt the model for shorter time resolution for more accurate results and to evaluate if that can make FCR-N trade even more beneficial.

Based on our research and historical data analysis, there is potential for financial gains for buildings engaging in explicit demand response in the daily FCR-N market. Additionally, it is worth noting that power storage was found to be cost-efficient only when combined with FCR trade. These results and the presented novel methodology for building hybrid energy system optimization offer researchers a valuable foundation for further exploration into the integration of demand response strategies and energy storage solutions in building design and operation. Moreover, they provide industry stakeholders with practical tools and information for implementing energy-efficient technologies that can not only increase cost-efficiency but also contribute to a greener energy landscape.

This study demonstrates that based on the current prices of PS used, economic feasibility for PS in hybrid energy systems is only achievable through participation in the FCR-N market. Without future price reductions on PS technologies, this remains the sole viable path. Future research should explore other Frequency Containment Reserve (FCR) products to assess their impact on the economic feasibility of PS in hybrid energy systems within buildings.

CRediT authorship contribution statement

Rebecka Savolainen: Conceptualization, Methodology, Validation, Formal analysis, Resources, Investigation, Data curation, Writing - original Draft. **Johannes Einolander:** Validation, Formal analysis, Resources. **Risto Lahdelma:** Conceptualization, Methodology, Validation, Resources, Writing - review & editing.

Declaration of competing interest

The authors declare the following financial interests/personal relationships which may be considered as potential competing interests: Nothing to declare. If there are other authors, they declare that they have no known competing financial interests or personal relationships that could have appeared to influence the work reported in this paper.

Data availability

Data will be made available on request.

Acknowledgment

We thank Granlund Ltd. and Fingrid Oyj for providing input data.

Appendix A. Yearly planning model

The yearly planning model is a modified version of the LP/MILP model presented in [47]. The planning model solves the optimal sizing and operation of the building energy system minimizing combined fixed and hourly operative costs for the energy supply units U = {PP, HP, DH} and storage units S = {HS, PS} over the time horizon $t = 1, \ldots, T$. When used for sizing, the time horizon is a full year with investment costs as annuities. Compared to the earlier model, this model excludes photovoltaic power and cooling, but the power storage model is more detailed. Also, here the configuration is fixed, i.e., inclusion or exclusion of different energy supplies and storages is not optimized using binary variables.

$$MinZ = \sum_{u\in U}\sum_{t=1}^{T} c_{u,t}x_{u,t} + \sum_{u\in U}\left(c_u^{MAX}x_u^{MAX} + c_u^{CONST}\right) + \sum_{u\in S}\left(c_u^{MAX}s_u^{MAX} + c_u^{CONST}\right) \tag{A.1}$$

$$x_{DH,t} + x_{HP,t}^{H} - s_{H,t}^{INOUT} = d_{H,t}, \tag{A.2}$$

$$x_{PP,t} - x_{HP,t} - s_{P,t}^{INOUT} = d_{P,t}\ t = 1, \ldots, T. \tag{A.3}$$

$$x_{HP,t}^{H} = \eta_{HP,t}x_{HP,t}, t = 1, \ldots, T, \tag{A.4}$$

$$0 \le x_{u,t} \le x_u^{MAX}, t = 1, \ldots, T, u \in \mathrm{U}, \tag{A.5}$$

$$s_{u,t} = \eta_u^S s_{u,t-1} + \eta_u^{IN} s_{u,t}^{IN} - s_{u,t}^{OUT} 1 \Big/ \eta_u^{OUT}, \tag{A.6}$$

$$s_u^{MIN} \leq s_{u,t} \leq s_u^{MAX}, \tag{A.7}$$

$$0 \leq s_{u,t}^{IN} \leq s_u^{IN,MAX}, 0 \leq s_{u,t}^{OUT} \leq s_u^{OUT,MAX}, \tag{A.8}$$

$$s_{u,t}^{INOUT} = s_{u,t}^{IN} - s_{u,t}^{OUT}, 1, \ldots, T, \tag{A.9}$$

$$s_{u,0} = s_{u,T}, u \in \mathrm{S}. \tag{A.10}$$

The objective function (A.1) minimizes the combined operating and fixed energy costs for the building. The first summation adds up operating costs over the hours in the planning horizon, second summation is the fixed costs for energy supply units, and the last summation is the fixed costs of storages. Heat and power balance constraints (A.2, A.3) state that energy supply minus net charging of storage must match the hourly demand. In A.4, the heat pump converts power into heat by an efficiency ratio $\eta_{HP,t}$ (COP-factor). The COP-factor depends on outdoor temperature in case of an air-source HP, but is typically constant for ground source HP. Constraints A.5 set capacity limits for all energy supply units: HP, DH, PP. Dynamic constraints (A.6) determine the storage level at end of each period based on previous storage level and charge&discharge during current period applying efficiency ratios η_u^S, η_u^{IN}, and η_u^{OUT} to model losses during storage, charge, and discharge, correspondingly. Constraints A.7, and A.8 limit the storage level and charge&discharge rates. The net charge rate (A.9) is the difference between charge rate and discharge rate. Unlike the other LP variables, the net charge rate can be negative. The initial and final storage levels $(s_{u,0}, s_{u,T})$ are set equal in A.10.

References

[1] X. Lü, T. Lu, S. Karirinne, A. Mäkiranta, D. Clements-Croome, Renewable energy resources and multi-energy hybrid systems for urban buildings in Nordic climate, Energ. Buildings 282 (2023) 112789, https://doi.org/10.1016/j.enbuild.2023.112789.

[2] Z. Guowen, B. Mingliang, Z. Xinyu, L. Jiajia, L. Qiang, L. Jinfu, Y. Daren, Study on the distribution characteristics and uncertainty of multiple energy load patterns for building group to enhance demand side management, Energ. Buildings 263 (2022) 112038, https://doi.org/10.1016/j.enbuild.2022.112038.

[3] X. Zhang, J.L. Ramírez-Mendiola, Y. Lai, J. Su, M. Li, L. Guo, Optimization of demand response-oriented electrolytic and fuel cell cogeneration system for community residents: Uncovering flexibility and gaps, Energy Conversion and Management 287 (2023) 117099, https://doi.org/10.1016/j.enconman.2023.117099.

[4] ENTSO-E, Electricity balancing in Europe. Balancing Guide. November 2018 (pdf), 2018.

[5] A. Khodadadi, L. Herre, P. Shinde, R. Eriksson, L. Söder, M. Amelin, Nordic balancing markets: Overview of market rules, in: 2020 17th Int. Conf. Eur. Energy Mark, IEEE, 2020, pp. 1–6, https://doi.org/10.1109/EEM49802.2020.9221992.

[6] ENTSO-E, Fast Frequency Reserve – Solution to the Nordic inertia challenge (pdf), 2019.

[7] M. Gomez-Gonzalez, J.C. Hernandez, D. Vera, F. Jurado, Optimal sizing and power schedule in PV household-prosumers for improving PV self-consumption and providing frequency containment reserve, Energy 191 (2020) 116554, https://doi.org/10.1016/j.energy.2019.116554.

[8] C. Betzin, H. Wolfschmidt, M. Luther, Electrical operation behavior and energy efficiency of battery systems in a virtual storage power plant for primary control reserve, Int J of El Power & En Sys 97 (April 2018) 138–145, https://doi.org/10.1016/j.ijepes.2017.10.038.

[9] Finnish TSO Fingrid. Electricity markets. Frequency containment reserves (FCR-N, FCR-D), transactions in the hourly and yearly markets. (Accessed 15.8.2021).

[10] J.C. Hernandez, F. Sanchez-Sutil, F.J. Muñoz-Rodríguez, Design criteria for the optimal sizing of a hybrid energy storage system in PV household-prosumers to maximize self-consumption, Energy 186 (2019) 115827, https://doi.org/10.1016/j.energy.2019.07.157.

[11] E.M. Urbano, V. Martinez-Viol, K. Kampouropoulos, L. Romeral, Energy equipment sizing and operation optimisation for prosumer industrial SMEs – a lifetime approach, Appl. Energy 299 (2021) 117329, https://doi.org/10.1016/j.apenergy.2021.117329.

[12] H. Wang, S. Wang, R. Tang, Development of grid-responsive buildings: opportunities, challenges, capabilities and applications of HVAC systems in non-residential buildings in providing ancillary services by fast demand responses to smart grids, Appl. Energy 250 (2019) 697–712, https://doi.org/10.1016/j.apenergy.2019.04.159.

[13] M. Farrokhifar, A.H. Farid Aghdam, A. Alahyari, A. Monavari, A. Safari, Optimal energy management and sizing of renewable energy and battery systems in residential sectors via a stochastic MILP model, Electr. Pow. Syst. Res. 187 (2020) 106483, https://doi.org/10.1016/j.epsr.2020.106483.

[14] S. Rotger-Griful, R. Hylsberg Jacobsen, D. Nguyen, G. Sørensen, Demand response potential of ventilation systems in residential buildings, Energ. Buildings 121 (2016), https://doi.org/10.1016/j.enbuild.2016.03.061.

[15] H. Tang, S. Wang, A model-based predictive dispatch strategy for unlocking and optimizing the building energy flexibilities of multiple resources in electricity markets of multiple services, Appl. Energy 305 (2022) 117889, https://doi.org/10.1016/j.apenergy.2021.117889.

[16] A. Ramos, M. Tuovinen, M. Ala-Juusela, Battery energy storage system (BESS) as a service in Finland: business model and regulatory challenges, Journal of Energy Storage 40 (2021) 102720, https://doi.org/10.1016/j.est.2021.102720.

[17] A. Boldrini, J.P. Jim`enez Navarro, W.H.J. Crijns-Graus, M.A. van den Broek, Renewable and Sustainable Energy Reviews 154, 2022, p. 111853, https://doi.org/10.1016/j.rser.2021.111853.

[18] T. Tukia, S. Uimonen, M. Lehtonen, Evaluating the applicability of elevators in frequency containment reserves, 15th Int. Conf. Eur. Energy Mark., IEEE (2018) 1–5, https://doi.org/10.1109/EEM.2018.8469827.

[19] S. Uimonen, T. Tukia, M.-L. Siikonen, M. Lehtonen, Potential of aggregated escalator loads in demand response, Electr. Pow. Syst. Res. 175 (2019) 105917, https://doi.org/10.1016/j.epsr.2019.105917.

[20] J. Fleer, S. Zurmühlen, J. Meyer, J. Badeda, P. Stenzel, J.-F. Hake, D.U. Sauer, Techno-economic evaluation of battery energy storage systems on the primary control reserve market under consideration of price trends and bidding strategies, Journal of Energy Storage 17 (2018) 345–356, https://doi.org/10.1016/j.est.2018.03.008.

[21] S.P. Melo, U. Brand, T. Vogt, J.S. Telle, F. Schuldt, K.V. Maydell, Primary frequency control provided by hybrid battery storage and power-to-heat system, Appl. Energy 233–234 (2019) 220–231, https://doi.org/10.1016/j.apenergy.2018.09.177.

[22] T. Kaschub, P. Jochem, W. Fichtner, Solar energy storage in German households: profitability, load changes and flexibility, Energy Policy 98 (2016) 520–532, https://doi.org/10.1016/j.enpol.2016.09.017.

[23] L.C. Casals, M. Barbero, C. Corchero, Reused second life batteries for aggregated demand response services, J. Clean. Prod. 212 (99–108) (2019), https://doi.org/10.1016/j.jclepro.2018.12.005.

[24] P. Pandžić, I. Pavić, I. Androćec, H. Pandžić, Optimal battery storage participation in European energy and reserves markets, Energies 13 (6629) (2020), https://doi.org/10.3390/en13246629.

[25] Wang F, Zhou L, Ren H, Liu X, Talari S, Shafie-Khah M, Catalão, J.P.S. Multi-objective optimization model of Source–load–storage synergetic dispatch for a building energy management system based on TOU Price demand response. IEEE Trans. Ind. Appl., 54, 1017–1028; https://doi.org/10.1109/TIA.2017.2781639.

[26] J. Posma, I. Lampropoulos, W. Schram, W. Van Sark, Provision of ancillary services from an aggregated portfolio of residential heat pumps on the Dutch frequency containment reserve market, Appl. Sci. 9 (590) (2019), https://doi.org/10.3390/app9030590.

[27] A. Lesage-Landry, H. Wang, I. Shames, Online convex optimization of multi-energy building-to-grid ancillary services, IEEE Trans Control Syst Technol 28 (6) (November 2020), https://doi.org/10.1109/TCST.2019.2944328.

[28] P. Astero, C. Evens, Optimum operation of battery storage system in frequency containment reserves markets, IEEE Transactions on Smart Grid. 11 (6) (Nov. 2020), https://doi.org/10.1109/TSG.2020.2997924.

[29] A. Vannoni, A. Source, Integrated energy and ancillary services optimized management and risk analysis within a pay-as-bid market, Appl. Energy 371 (2024) 123628, https://doi.org/10.1016/j.apenergy.2024.123628.

[30] D. Cremoncini, G.F. Frate, A. Bischi, T.T. Pedersen, G.B. Andresen, A. Bentien, L. Ferrari, Optimal participation of a wind and hybrid battery storage system in the day-ahead and automatic frequency restoration reserve markets, Journal of Energy Storage 94 (2024) 112309, https://doi.org/10.1016/j.est.2024.112309.

[31] R. Subramanya, M. Yli-Ojanperä, S. Sierla, T. Hölttä, J. Valtakari, V. Vyatkin, A virtual power plant solution for aggregating photovoltaic systems and other distributed energy resources for northern European primary frequency reserves, Energies 14 (1242) (2021), https://doi.org/10.3390/en14051242.

[32] O. Terreros, J. Spreitzhofer, D. Basciotti, R.R. Schmidt, T. Esterl, M. Pober, Electricity market options for heat pumps in rural district heating networks in Austria, Energy 196 (116875) (2020), 10.1016/j.

[33] J. Tan, Q. Wu, M. Zhang, Strategic investment for district heating systems participating in energy and reserve markets using heat flexibility, Int. J. Electr. Power Energy Syst. 137 (2022) 107819, https://doi.org/10.1016/j.ijepes.2021.107819.
[34] N. Javanshir, S. Syri, S. Tervo, A. Rosin, Operation of district heat network in electricity and balancing markets with the power-to-heat sector coupling, Energy 266 (2023) 126423, https://doi.org/10.1016/j.energy.2022.126423.
[35] F. Iov, M. Khatibi, J.D. Bendtsen, On the participation was presented and of power-to-heat assets in frequency regulation markets—a Danish case study, Energies (2020) 13, https://doi.org/10.3390/en13184608.
[36] S. Lotfi, M. Sedighizadeh, R. Abbasi, S.H. Hosseinian, Vehicle-to-grid bidding for regulation and spinning reserve markets: a robust optimal coordinated charging approach, Energy Rep. 11 (2024) 925–936, https://doi.org/10.1016/j.egyr.2023.12.044.
[37] Wang Z, Hou S. Optimal participation of battery swapping stations in frequency regulation market considering uncertainty.
[38] Seo M, Jin Y, Kim M, Son H, Han S. Strategies for electric vehicle bidding in the German frequency containment and restoration reserves market. Electric Power Systems.
[39] J. Einolander, A. Kiviaho, R. Lahdelma, Impact of V2G, V2H and FCR to Electricity Costs of Households with Varying Primary Heating Sources, in: 2023 IEEE Int. Intell. Transp. Syst. Conf, 2023.
[40] J. Einolander, R. Lahdelma, Multivariate copula procedure for electric vehicle charging event simulation, Energy (2021) 121718, https://doi.org/10.1016/j.energy.2021.121718.
[41] P. Astero, C. Evens, Optimum day-ahead bidding profiles of electrical vehicle charging stations in FCR markets, Electr. Pow. Syst. Res. 190 (2021), https://doi.org/10.1016/j.epsr.2020.106667.
[42] J. Einolander, A. Kiviaho, R. Lahdelma, Household Electricity Cost Optimization with Vehicle to-Home Technology and Mixed-Integer Linear Programming. Int. Conf. Futur. Energy Solut., Vaasa, Finland: IEEE, 2023, https://doi.org/10.1109/FES57669.2023.10182713.
[43] J. Einolander, R. Lahdelma, Explicit demand response potential in electric vehicle charging networks: event-based simulation based on the multivariate copula procedure, Energy 256 (2022) 124656, https://doi.org/10.1016/j.energy.2022.124656.
[44] C. Utama, S. Troitzsch, J. Thakur, Demand-side flexibility and demand-side bidding for flexible loads in air-conditioned buildings, Appl. Energy 285 (2021) 116418, https://doi.org/10.1016/j.apenergy.2020.116418.
[45] Stanislaw L, Seatle M, McPherson M. Quantifying the value of building demand response: Introducing a cross-sectoral model framework to optimize demand response scheduling.
[46] C.D. Korkas, M. Terzopoulos, C. Tsaknakis, E.B. Kosmatopoulos, Nearly optimal demand side management for energy, thermal, EV and storage loads: An Approximate Dynamic Programming approach for smarter buildings, Energy and Buildings 255 (2022) 111676, https://doi.org/10.1016/j.enbuild.2021.111676.
[47] R. Rikkas, R. Lahdelma, Energy supply and storage optimization for mixed-type buildings, Energy 231 (2021) 120839, https://doi.org/10.1016/j.energy.2021.120839.
[48] R. Savolainen, R. Lahdelma, Optimization of renewable energy for buildings with energy storages and 15-minute power balance, Energy 243 (2022) 123046, https://doi.org/10.1016/j.energy.2021.123046.
[49] H. Wang, S. Wang, K. Shan, Experimental study on the dynamics, quality and impacts of using variable-speed pumps in buildings for frequency regulation of smart power grids, Energy 199 (2020) 117406, https://doi.org/10.1016/j.energy.2020.117406.
[50] D. Yousri, H. Farag, H. Zeineldin, E. El-Saadany, Integrated model for optimal energy management and demand response of microgrids considering hybrid hydrogen-battery storage systems, Energy Conversion and Management 280 (2023) 116809, https://doi.org/10.1016/j.enconman.2023.116809.
[51] J. Koskela, A. Rautiainen, P. Järventausta, Using electrical energy storage in residential buildings – sizing of battery and photovoltaic panels based on electricity cost optimization, Appl. Energy 239 (2019) 1175–1189, https://doi.org/10.1016/j.apenergy.2019.02.021.
[52] Tesla Powerpack System Datasheet (pdf). Available at, www.impulsora.com, 2020 (Assessed 1.7.2021).
[53] Helen Ltd, Electricity distribution prices, Available at, https://www.helensahkoverkko.fi/en/services/electricity-distribution-prices (Assessed 2.8.2021).
[54] R. Lahdelma, G. Kayo, E. Abdollahi, P. Salminen, Optimization and multicriteria evaluation of district heat production and storage, in: In book: New Perspectives in multiple criteria decisions making, 2019, https://doi.org/10.1007/978-3-030-11482-4_15, p. 371e96.
[55] Solrico, Solar thermal world organization. Bärbel E. Seasonal pit heat storage: cost benchmark of 30 EUR/m^3, 2019.
[56] Helen Ltd. District heat prices. Available at District heat prices | Helen (Assessed 2.8.2021).
[57] Nord Pool Spot, Hourly data Elspot. Historical Market Data. Elspot prices. Available at Historical Market Data | Nord Pool. nordpoolgroup.com (Assessed 2.8.2021).
[58] Finnish TSO Fingrid, The technical requirements and the prequalification process of Frequency Containment Reserves 2022 (version May 6, 2022 pending approval of legal methodology). https://www.fingrid.fi/en/electricity-market/reserves_and_balancing/frequency-containment-reserves/introduction-of-new-technical-requirements-for-frequency-containment-reserves/ (Accessed 17.6.2022).
[59] S. Oksanen, Participation in Ancillary Service and Physical Electricity Markets with Flexible Demand Resources, Master's Thesis, Aalto University, 2017. Available at, https://aaltodoc.aalto.fi/bitstream/handle/123456789/27088/master_Oksanen_Santeri_2017.pdf?sequence=1&isAllowed=y (Accessed 12.7.2021).
[60] Finnish TSO Fingrid, Development project for aggregation on the reserve market. 2016, Available at, https://www.fingrid.fi/en/pages/news/news/2016/development-project-for-aggregation-on-the-reserve-market–aiming-at-a-cost-efficient-and-flexible-electricity-system/, 2016 (Accessed 19.7.2021).
[61] Finnish TSO Fingrid, Electricity markets. Reserves and balancing market. Frequency containment reserves, Available at, https://www.fingrid.fi/en/electricity-market/reserves_and_balancing/frequency-containment-reserves/ (Accessed 19.7.2021).
[62] T. Fang, R. Lahdelma, Optimization of combined heat and power production with heat storage based on sliding time window method, Appl. Energy 162 (2016) 723–732, https://doi.org/10.1016/j.apenergy.2015.10.135.
[63] R. Lahdelma, H. Hakonen, An efficient linear programming algorithm for combined heat and power production, Eur. J. Oper. Res. 148 (2003) 141–151, https://doi.org/10.1016/S0377-2217(02)00460-5.
[64] I. Mathews, B. Xu, W. He, V. Barreto, T. Buonassisi, I.M. Peters, Technoeconomic model of second-life batteries for utility-scale solar considering calendar and cycle aging, Appl. Energy 269 (2020) 115127, https://doi.org/10.1016/j.apenergy.2020.115127.